Results in Chemistry 3 (2021) 100193

Contents lists available at ScienceDirect

Results in Chemistry

journal homepage: www.sciencedirect.com/journal/results-in-chemistry

A *N*-(4-chlorophenyl)-γ-amino acid derivatives exerts *in vitro* anticancer activity on non-small cell lung carcinoma cells and enhances citosine arabinoside (AraC)-induced cell death via mitochondria-targeted pathway

Povilas Kavaliauskas [a,b,c,d,e,*], Šarūnas Žukauskas [d], Kazimieras Anusevičius [d], Benas Balandis [d], Rita Vaickelionienė [d], Vidmantas Petraitis [a,b,e], Vytautas Mickevičius [b,d]

[a] Joan and Sanford I. Weill Department of Medicine, Weill Cornell University, 1300 York Avenue, NY 1109. New York, United States
[b] Institute of Infectious Diseases and Pathogenic Microbiology, Birštono str. 38A, Prienai LT-59116, Lithuania
[c] University of Maryland, School of Medicine, 655 W. Baltimore Street, Baltimore, MD 21201, United States
[d] Kaunas University of Technology, Radvilėnų rd. 19, Kaunas LT-50254, Lithuania
[e] Biological Research Center, Lithuanian University of Health Sciences, Tilzes str. 18, Kaunas LT-47181, Lithuania

ARTICLE INFO

Keywords:
Amino acids
Azole
Diazole
Triazole
Anticancer activity
Lung cancer
Non-small cell carcinoma
Drug repurposing
ROS

ABSTRACT

A Non-Small Cell Lung Cancer (NSCLC) is among the leading cause of cancer-associated morbidity and mortality worldwide. Novel treatment and drug repurposing strategies are needed. Cytosine arabinoside (AraC) is an S-phase inhibitor historically used for the treatment of leukemia. Previously AraC was not investigated as a therapeutic option for NSCLC. We explored a novel adjuvant therapy concept *in vitro* targeting S-phase and mitochondrial pathways. A synthetic pathway to generate novel mitochondria damaging N-(4-chlorophenyl)-γ-amino acid derivatives bearing an azole, diazole and triazole moieties was described. The resulting compounds were evaluated for their anticancer activity on well described A549 cells. Five compounds demonstrated convincing anticancer activity comparable to cytosine arabinoside (AraC). The most promising compound **7g** (IC_{50} = 38.38 μM) bearing 3,4-dichlorophenyl moiety was able to induce the mitochondrial injury, leading to significant ($p < 0.05$) ROS production and inhibition of ATP synthesis. **7g** synergized with AraC and significantly decreased A549 viability in comparison to AraC and **7g** monotherapy or UC. The cytotoxic effect on A549 viability after AraC combination with **7g** was similar to doxorubicin monotherapy. These results suggest that **7g** could be potentially explored adjuvant enhancing the activity of standard chemotherapeutic agents. Further studies are needed to better understand the safety, efficacy, and precise cellular targets of of N-(4-chlorophenyl)-γ-amino acids.

Introduction

Lung cancer remains the leading causes of malignancy-associated deaths worldwide [1]. Non-Small Cell Lung Cancer (NSCLC) is the most common cancer type affecting the pulmonary system [2]. In many patients, NSCLC represents locally advanced or even metastatic diseases therefore limiting the currently available treatment option. Standard chemotherapy with clinically approved cytostatic and cytotoxic drugs is often beneficial for NSCLC patients; however, NSCLC may acquire multiple resistance mechanisms leading to altered management and poor treatment prognosis. Furthermore, advanced-stage, metastatic and chemotherapy-resistant NSCLC often requires aggressive treatment strategies using high doses of cytotoxic agents, therefore increasing risk in development of chemotherapy-associated systemic toxicity [3]. The profound chemotherapy-associated toxicity can be reduced by establishing adjuvant-based treatment strategies by combining two or more cytostatic or cytotoxic compounds with synergistic interactions against NSCLC [4].

Cell cycle-specific chemotherapy drugs are common type of anticancer chemotherapy that are used to treat number of various cancers, including NSCLC. The cell cycle specific drugs works by interacting with specific steps of cell cycle leading to the induction of apoptosis and death of transformed cells. Cancerous cells often acquire series of mutations leading to the ability to resist the cell cycle inhibitors [5–7]. Therefore, a

* Corresponding author at: Joan and Sanford I. Weill Department of Medicine, Weill Cornell University, 1300 York Avenue, NY 1109. New York, United States.
E-mail address: pok4001@med.cornell.edu (P. Kavaliauskas).

https://doi.org/10.1016/j.rechem.2021.100193
Received 5 May 2021; Accepted 15 September 2021
Available online 27 September 2021

novel drug repurposing and combinational strategies are needed to target rapidly emerging chemotherapy resistance in various neoplasms [8–10].

Cytosine arabinoside (AraC) is a known and clinically well tolerated S phase inhibitor targeting to the DNA synthesis in rapidly growing cells [11]. AraC is often used alone and in combinations with other chemotherapy drugs to treat acute leukemia [12]. The use of AraC for the treatment or control of NSCLC have not been investigated before. Cancerous cells that entered S phase are highly susceptible for the nutrient starvation and ROS induced-DNA damage. Therefore, combinational approach of using AraC as S cycle inhibitor and compounds inducing ROS could be potentially beneficial for the control of the chemotherapy resistant or advanced NSCLC.

Mitochondria play a vital role in cancer pathogenesis and are considered as potential target for anticancer therapy [13]. Differently than normal cells, the cancer cells are known for their ability to generate reactive oxygen forms (ROS) and increased levels of adenosine triphosphate (ATP) by harnessing aerobic glycolysis known as Warburg effect [14]. Transformed cells have increased metabolic needs, therefore opening window for novel mitochondria-targeted therapies. Besides that, the overall ROS levels are overall greater in cancer cells, therefore modulating cellular ROS pathway could potentially enhance cytotoxic activity of standard chemotherapy by inducing mitochondria-depended apoptosis or mitophagy [15].

The combinational approach of using cytotoxic drugs and mitochondria-accumulating compounds could be potentially explored as adjuvant strategy for controlling systemic chemotherapy-associated toxicity [16]. Previous mitochondria-targeting approaches were based on conjugation of mitochondria-accumulating ligands with known anticancer drugs [17,18]. Besides that, several mitochondria-targeting small molecules with promising anticancer activity have been previously described and investigated [19,20]. Heterocyclic compounds play a pivotal role in the biological processes of all living organisms [21]. Many pharmacologically active compounds share various heterocyclic moieties. Various five-membered heterocyclic compounds, containing one or more nitrogen atoms exhibit profound biological activity. Among biologically active heterocycles, pyrrole, pyrazole and triazole cycles are commonly used to generate compounds bearing anticancer, antimicrobial and various inhibitory properties [22–25]. Therefore, compounds bearing various heterocyclic substitutions could be potentially explored as novel therapeutics.

The anticancer activity of pyrrole-containing compounds is mostly based on the direct inhibition of Epidermal Growth Factor (EGFR) and Vascular Endothelial Growth Factor (VEGFR) receptors or various kinases [26,27]. Kaspersen *et al.* reports a synthesis of selective and active EGFR tyrosine kinase inhibitors based on 4-*N*-substituted 6-aryl-7*H*-pyrrolo[2,3-*d*]pyrimidine-4-amines. The novel pyrrole derivatives exhibited good inhibitory and anticancer activity by targeting downstream EGFR pathway [26]. Furthermore, the study of La Regina *et al.* described a synthesis and biological characterization of novel pyrrole-containing compounds targeting cellular tubulin polymerization, migration, and intracellular trafficking [28]. Beside the inhibitory activity on EGFR, VEGFR and tubulin, by Boukouvala *et al.* have demonstrated that several pyrrole derivatives are able to interfere with mitochondrial carbon metabolism, leading to the induction of mitochondria-depended cell death [29,30]. Therefore, pyrrole containing compounds should be explored as promising anticancer and mitochondria-targeting compounds.

Pyrazoles, the representatives of diazoles, are rarely found in nature, however, synthetic analogues display multifarious biological activities [31–33]. Pyrazole moieties bearing compounds have long been investigated as potential anticancer compounds [34–37]. Abdelgawad *et al.* reported that the incorporation of pyrazole scaffold greatly improved the antiproliferative activity of benzimidazole derivatives [34]. Pellei *et al.* reported pyrazole containing organo-copper compounds with potential anticancer properties [38]. Marani *et al.* described the synthesis biological activity of pyrazolopyran derivatives with inhibitory activity of cytosolic hydroxymethyltransferase [39] (SHMT1). Cytosolic SMHT1 shares a homology with mitochondrial enzyme SHMT2, therefore various pyrrole derivatives could potentially be used as a mitochondrial SHMT2 inhibitors and useful for treatment of metastatic neoplasms. Furthermore, various pyrazoles have been shown to disrupt mitochondrial membrane potential, modulate Bax and Bcl-2 protein levels and induce apoptosis in NSCLC cells by activating caspase-3 [33].

Triazoles have been already successfully implemented in clinics or under clinical trials for the treatment of various malignancies and other disorders (Fig. 1). The incorporation of various triazole linkers bearing anticancer pharmacophores greatly improving the anticancer and antiproliferative activity of the compounds [40,41]. The cytostatic activity of triazole containing compounds is often based on the inhibition of EGFR, BRAF, and tubulin pathways [41,42]. Several triazoles nucleus containing compounds have been shown to have strong antiproliferative and apoptosis-inducing activity by targeting thymidine phosphorylase, making triazole containing compounds attractive for treatment NSCLC [40]. Furthermore, Omar *et al.* describes a synthesis of novel water-soluble and mitochondria-targeting osmium triazole complexes with micromolar cytotoxic activity on HeLa cells [43]. The compounds were readily absorbed in mitochondria and after activation with light were able to induce the cell death by ROS generation. Favorable pharmacokinetics and selective cytotoxicity displayed by various triazoles makes them attractive pharmacophores for development of compounds targeting various lung cancers [44].

γ-Aminobutyric acid (GABA) is a cell permeable inhibitory neurotransmitter highly abundant in mammalian central nervous system (CNS). Beside directly acting on CNS, GABA and its derivatives have previously showed to be involved in the regulation of cancer proliferation by directly acting on mitogen-activated protein kinase (MAPK) signalling pathways [45]. Like the GABA itself, various derivatives have great biological and pharmacological significance (Fig. 2). Due to good absorption and ability to cross brain-blood barrier many GABA-based compounds have good tissue distribution and activity on CNS.

Various neurotransmitters have been previously reported to be involved in the initiation and progression of colon tumors [46,47]. GABA receptors are highly expressed in various tumors and their regulatory role in tumor migration and metastasis was experimentally confirmed by several researchers [48,49]. Therefore, pharmacological modulation of GABA receptors using various GABA derivatives could have profound anticancer and anti-metastatic activity.

The wide spectrum in biological activity of γ-amino acid and heterocycle motifs containing compounds makes them attractive building blocks in the development of novel and mitochondria-targeting antiproliferative agents. With this notion, we aimed to synthesize and evaluate the biological and synergistic activity of novel mitochondria-targeting *N*-substituted γ-amino acid derivatives bearing functionalized azole, diazole, triazole, thiazole-triazole moieties on human non-small cell carcinoma cells.

Results and discussion

Synthesis and characterization of N-(4-chlorophenyl)-γ-amino acid derivatives bearing an azole, diazole and triazole moieties

Herein we report the synthesis and biological properties of a series of novel *N*-(4-chlorophenyl)-γ-amino acid derivatives (Scheme 1). 1,2,4-Triazolethione derivative **1** was obtained according to the method described in [50,51] and applied for the preparation of **2** [50]. The obtained cyclic compound 1-(4-chlorophenyl)-4-(5-thioxo-4,5-dihydro-1*H*-1,2,4-triazol-3-yl)pyrrolidin-2-one (**1**) was treated with ethyl chloroacetate in 1,4-dioxane. The alkylation reaction occurred fairly easily and after the dilution of the reaction mixture with water the desired product ethyl ({3-[1-(4-chlorophenyl)-5-oxopyrrolidin-3-yl]-1*H*-1,2,4-triazol-5-yl}sulfanyl)acetate (**2**) was isolated.

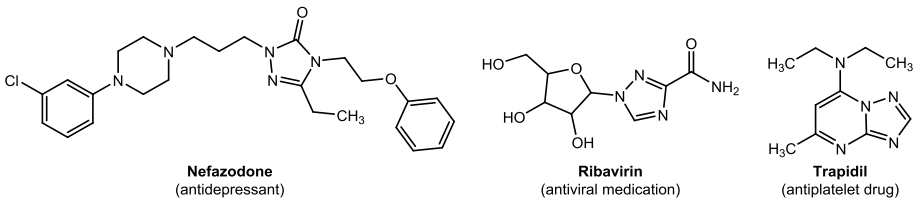

Fig. 1. Pharmaceuticals based on 1,2,4-triazole scaffold.

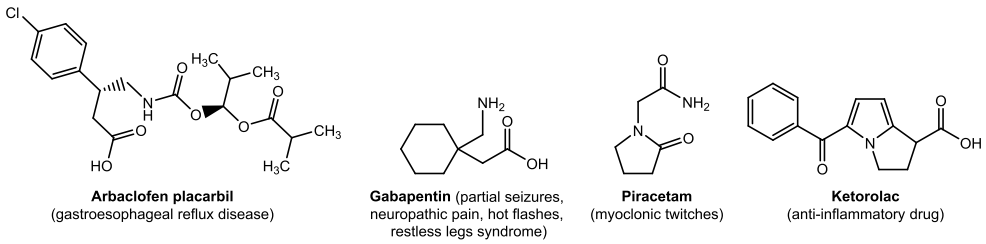

Fig. 2. Pharmaceuticals with the γ-aminobutyric acid fragment in their structure.

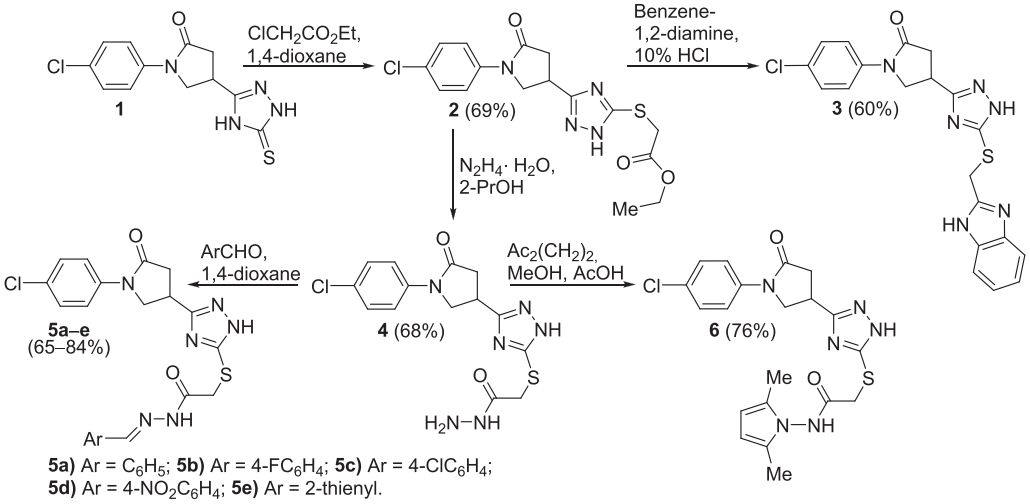

Scheme 1. Synthesis and chemical transformations of S-alkylated products **2**–**6.**

The interaction of ethyl esters **2** with benzene-1,2-diamine in 10% aqueous hydrochloric acid for 48 h afforded compound **3** with benzimidazole moiety in the molecule. The target derivative **3** was isolated from the reaction mixture by diluting it with water.

The reaction of ester **2** with hydrazine monohydrate was carried out under ordinary conditions, and the obtained acid hydrazide **4** was undergone various chemical transformations.

The hydrazide moiety is a convenient functional group for the coupling with aldehydes or ketones through a dehydration reaction to form hydrazone linkage. Hence the reactions of compound **4** with appropriate aromatic aldehydes and thiophene-2-carbaldehyde proceed fairly quickly resulting in the formation of hydrazones **5a–e** which, as expected, in DMSO-d_6 solution exists as a mixture of *Z*/*E* isomers, in which *Z* isomer predominates [52,53]. An interaction of hydrazide **4** with hexane-2,5-dione in methanol catalysed by acetic acid led to the cyclization product 2,5-dimethylpyrrole derivative **6**.

The alkylation of 1,2,4-triazolethione **1** with substituted α-haloketones in acetone at reflux showed that the reaction results in the formation of open chain non-condensed compounds **7a—l** in 51–97% yield (Scheme 2). The above-mentioned compounds **7a–l** were then

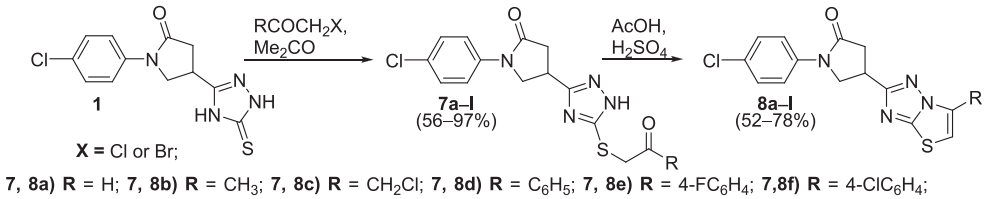

Scheme 2. Synthesis of *S*-alkylated products **7** and thiazolotriazoles **8.**

readily cyclized to the thiazolo[3,2-*b*][1,2,4]triazoles **8a–l** containing fused ring system in the structure by refluxing the corresponding starting compoud **7** for 3–12 h in acetic acid with the addition of a catalytic amount of sulfuric acid.

The formation of 2-oxoethylsulfanyl fragment in the structure of compounds **7a**−**l** can be demonstrated by comparison of the ^{1}H NMR spectra of compounds **1** and **7d**. The singlet at 4.82 ppm was assigned to the protons of the SCH_2CO moiety and the additional peaks integrated for five protons were attributing to the newly attached aromatic ring. The obvious differences in the ^{13}C NMR spectra of the mentioned compounds are also observed. The absence of the resonance line of C = S in the ^{13}C NMR spectrum of **7d**, which usually arise in the range of 168–167 ppm for triazolethiones, and peaks at 33.7 ($S\underline{C}H_2CO$) and 193.8 ($SCH_2\underline{C}O$) ppm, and the additional resonances in the aromatic region of the spectrum show the presence of the $SCH_2C(O)Ar$ moiety.

Biological activity evaluation

In silico ADME properties of N-(4-chlorophenyl)-γ-amino acid derivatives

The Absorption, Distribution, Metabolism and Excretion (ADME) properties of compounds **7, 8a–l** was estimated by using SwissADME software with default parameters [54]. The Lipinski rule of five was used to evaluate the drug-likeness of the synthesized compounds. The compounds with molecular mass lover than 500 g/mol, high lipophilicity (LogP > 5), <5 hydrogen bond donors, <10 hydrogen bond acceptors, molar refractivity between 40 and 130 were considered as drug-like.

The molecular weight of synthesized compounds ranged from 332.81 to 491.79 g/mol. The lipophilicity of the synthesized compounds ranged from 2.22 to 4.88 LogP. Hydrogen bond donors ranged from 0 to 1, while hydrogen bond acceptor number ranged from 3 to 6. The total polar surface area (TPSA) of the compounds **7, 8a–l** ranged from 78.74 to 150.07 Å^2, respectively (Table S1). **M** The investigated compounds were predicted to have moderate to poor water solubility, relatively good gastrointestinal (GI) absorption and low skin permeability (-9.3 to −5.41 Log Kp) making them as promising oral chemotherapeutic agents. All synthesized compounds except **8a** were predicted to be impermeable thought brain-blood barrier (Table S2). Based on the Lipinski rule of five, and predicted *in silico* ADME properties, the compounds were predicted to show good drug-likeness properties.

The excretion and metabolism properties of the compounds **7, 8a–l** were also estimated. The *in silico* estimation provided insights on the interaction with human P-glicoprotein 1 (Pgp) and major cytochrome P450 drug metabolisim systems. Both Pgp and cytochrome P450 are crucial for metabolisim and excreation of the drugs. Moreover, various cytochrome P450 isoforms are involved in the metabolic activation of various pre-carcinogens and participates in the inactivation and activation of anticancer drugs and xenobiotics [55].Compounds **7a, 8c, 8d, 8e, 8f, 8g** were predicted to be a substrates of Pgp (Table S3). All compounds, exept **7a, 7h, 7i** and **8i** were predicted to inhibit CYP1A2. Beside **7a,** all other synthesized derivatives of *N*-(4-chlorophenyl)-γ-amino acid were predicted to be inhibitors of CYP2C9. No compounds were predicted to inhibit CYP2D6 cytochrome P450 system (Table S3).

These results demosntrates that the *N*-(4-chlorophenyl)-γ-amino acid derivatives have various, structure-depended interactions with major cytochrome P450 drug metabolisim systems.

N-(4-Chlorophenyl)-γ-amino acid derivatives demonstrated a structure and concentration-depended antiproliferative activity

Anti-proliferative and cytotoxic activity of novel *N*-(4-chlorophenyl)-γ-amino acid derivatives **7, 8a–l** bearing an azole, diazole and triazole moieties were tested against human NSCLC cells A549 using MTT assay [56,57]. The A549 cell line was used as a well characterized and translational model that was previously used by numerous studies to screen compounds and therapies against NSCLC. The treatment induced cytotoxicity was then compared with known G(2)/M cell cycle inhibitor doxorubicin (DOX) and S cycle inhibitor cytosine arabinoside (AraC).

To understand the cytotoxic activity of novel *N*-(4-chlorophenyl)-γ-amino acid derivatives, the compounds were first screened at fixed, biologically-relavant concentration (100 μM) to select the most potent leads. The A549 cells were exposed to the compounds or control drugs for 24 h to simulate the realistic and humanised regime required for cancer treatment.

Five out of sixteen screened compounds demonstrated good anti-proliferative activity on A549 cells by reducing the A549 viability by 50% in comparison to UC (Fig. 3). DOX demonstrated the highest cytotoxic activity by reducing the A549 ciability by 20%, while treatment with AraC resulted in 50% decrease of A549 viability. The compounds **8c, 7d, 7e, 7g,** and **8i** showed the highest anti-proliferative activity at the concentration of 100 μM and were further used for the studies.

The related compounds (**7b, 7c, 8a, 8b)** did not demonstrated good anti-proliferative activity, therefore further suggesting that the anti-proliferative activity of *N*-(4-chlorophenyl)-γ-amino acid derivatives is structure depended. The structure–activity relationship analysis of the investigated compounds **7, 8** has shown that (Fig. 3) the anticancer activity of the *S*-alkylated compounds **7a,b** and their cyclization products **8a, b** with non-aromatic substituents is low and almost uniform, while the chloromethyl group was introduced the activity of **7c** and **8c** is markedly different. This can be explained by the fact that the chloromethyl group in compound **8c** is significantly more active as an alkylating agent compared to the chloromethyl group in compound **7c** due to the action of the carbonyl moiety. Examination of the anticancer activity of S-alkylated products **7d–l** and their cyclization products **8d-l** with variously substituted aromatic substituents shows that in the absence of a substituent in the phenyl ring (compound **7d**) or when the substituent is not bulky (compounds **7e, g**) such compounds are characterized by higher anticancer activity compared to cyclization products **8d, e, g**. As the size of the substituent on the phenyl ring increases, another trend is observed - the anticancer activity of the cyclization products **8i–l** is higher compared to the S-alkylated products **7i–l**. After evaluating the biological activity of the tested compounds and the reliability of the data, compounds **7d, e, g** and **8c, i** were selected for further studies.

The A549 cells were further treated with increasing concentrations (0 – 200 μM) of the most promising compounds (**8c, 7d, 7e, 7g,** and **8i)** or cytotoxic controls (DOX and AraC) and the viability as well as long term survival assays were used to evaluate the anticancer activity.

All selected compounds demostrated the concentration-depended anticancer activity on A549 cells. **7g** demonstrated the strongest anti-prolierative activity (IC_{50} = 38.38 μM), followed by **8i** (IC_{50} = 39.6 μM), **7d** (IC_{50} = 41.28 μM) in comparison to AraC (IC_{50} = 53.0 μM) (Table 1). The doxorubicin demonstrated the highest anticancer activity on A549 cells with IC_{50} = 2.6 μM.

We further investigated weather the cytotoxic activity is more selective for cancerous cells. The non-cancerous Vero african green moneky kidney cells were treated with fixed concentration (100 μM) as described before. All tested compounds reduced Vero viability by aproximatelly 50% (Fig. 4). The **7g** demonstrated weaker cytotoxcix activity on Vero cells, in comparison to A549 NSCLC cells, suggesting the possible existence of NSCLC-speciffic targets for the **7g.**

The anticancer potency and treatment-induced changes in cell phenotype were further confirmed by Live/Dead assay (Fig. 4). The A549 cells were pretreated with fixed 50 μM concentration of **8c, 7d, 7e, 7g,** and **8i** to simulate the IC_{50} of AraC. The DMSO treated cells served as compound untreated control while AraC (50 μM) served as a cytotoxicity comparator. The selected promising *N*-(4-chlorophenyl)-γ-amino acid derivatives were able to induce the death of A549 cells as it was evident by the acumulation of ethidium bromide homodimer (Eth-D) in A549 cells after 24 h treatment. The compouds **7g** and **8i** demonstrated the highest cytotoxic activity in comparison to untreated control and AraC (Fig. 5).

Colectivelly, this data demonstrates a structure-depended and selective cytotoxic activity of *N*-(4-chlorophenyl)-γ-amino acid derivatives

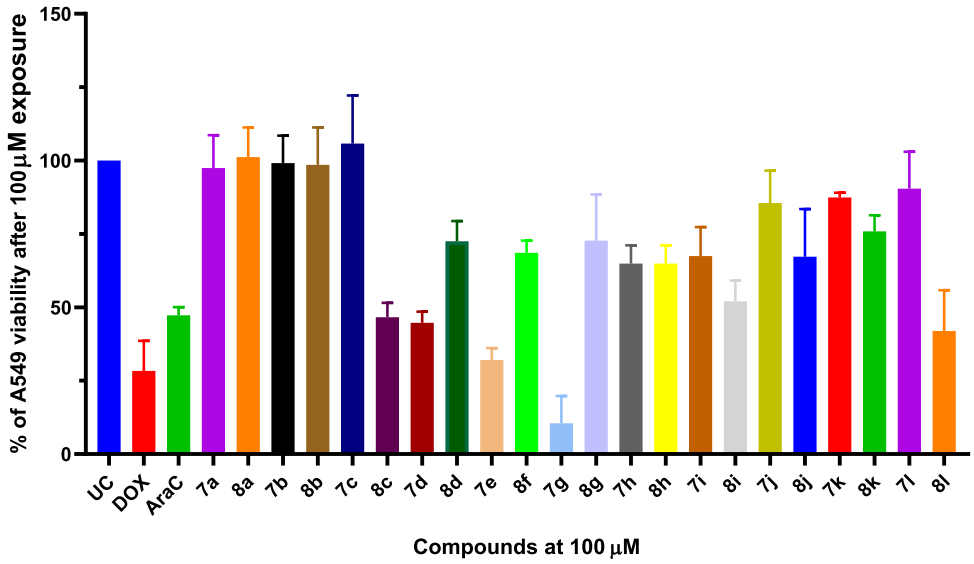

Fig. 3. The viability of A549 Non-Small Cell Lung Cancer cells after 24 h treatment with compounds **7, 8a–l** and reference drugs: doxorubicin (DOX) and cytosine arabinoside (AraC) with fixed concentration of 100 μM. The cell viability was evaluated by using MTT assay and % of viability was calculated from untreated control. Data shown are mean ± SD values from 3 separate experiments for each group.

Table 1
The anti-cancer activity of the most potent *N*-(4-chlorophenyl)-γ-amino acid derivatives and comparator drugs (doxorubicin, DOX and cytosine arabinoside, AraC) on human A549 lung carcinoma cells.

Compound	IC_{50} (μM)	R
7d	41.28	C_6H_5
7e	65.41	4-FC_6H_4
7g	38.38	3,4-$Cl_2C_6H_3$
8i	39.6	4-$(CF_3)C_6H_4$
8c	106.8	CH_2Cl
DOX	2.6	NA
AraC	53.0	NA

Abbreviations: R – radical, IC_{50} – Inhibitory concentration, DOX – doxorubicin, AraC – cytosine arabinoside.

on human A549 NSCLC cells. Compounds **7g, 8i** and **7d** showed the highest potency, suggesting the important role of phenyl radical in the cytotoxic activity. The 3,4-dichlorophenyl substituted ring in **7g** greatly improved the biological activity thus suggesting a this group as critical for cytotoxic activity.

The N-(4-chlorophenyl)-γ-amino acid derivatives are able to alter A549 colony formation

The cytotoxic assay based on A549 colony formation was performed to explore the effect of most potent compounds **8c, 7d, 8e, 7g** and **8i** on A549 cancer cell cytotoxicity (Fig. S46–50). All tested *N*-(4-chlorophenyl)-γ-amino acid derivatives were able to signifficantly ($*p < 0.05$) reduce the A549 viability in comparison to the untreated control (UC) (Fig. S46-50B). All selected compounds were able to alter the formation *in vitro* thus further supporting their cytotoxic and cytostatic activity.

The compound **8c** bearing the chloromethyl substituent demonstrated promising cytotoxic activity on A549 cells and was able to suppress the colony formation by concentration-depended manner. A549 exposed with 50 μM of **8c** was able to fully suppress the colony formation (Fig. S46 A, C) and significantly reduce the A549 viability ($p < 0.05$) in comparison to the untreated control Fig. S46 B). The activity of **8c** could be partly explained by the ability of chloromethyl compound act as alkylating agent. Furthermore, the compounds **7d** and **7e** bearing C_6H_5 and 4-FC_6H_4 radicals demonstrated similar activity on A549 colony formation as well as proliferation inhibition (Fig. S47, S48 A-C). Interestingly, despite high antiproliferative activity of **8i** (Fig. S50 B), the compound failed to greatly affect the colony formation of A549 cells (Fig. 50 A, C) thus exerting mostly cytostatic and non-cytoxic activity.

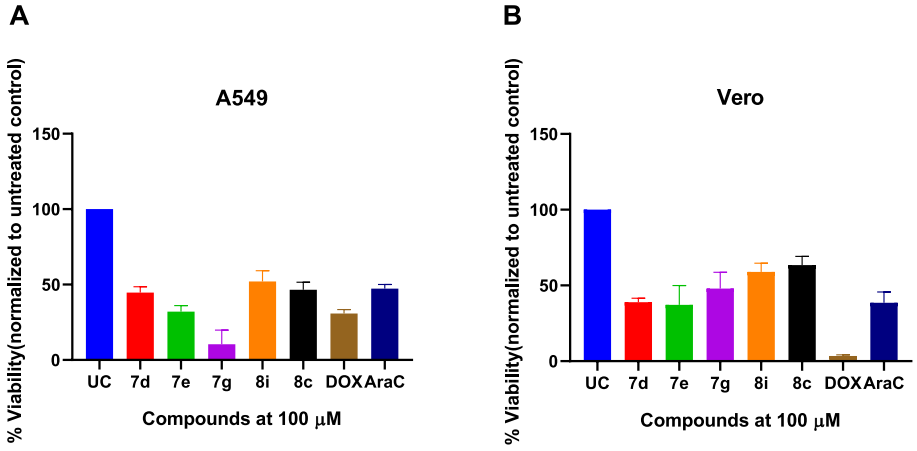

Fig. 4. The selected and most proising *N*-(4-chlorophenyl)-γ-amino acid derivatives **8c**, **7d**, **7e**, **7g**, and **8i** demonstrated the higher cytoxic activity on A549 than non-cancerous Vero cells. The A549 and Vero cells were treated with selected compounds or cytotoxicity comparators (doxorubicin, DOX, cytosine arabinoside, AraC) for 24 h at the fixed concentration of 100 μM. After the treatment, the viability was evaluated using MTT assay. Data shown are mean ± SD values from 3 separate experiments for each group.

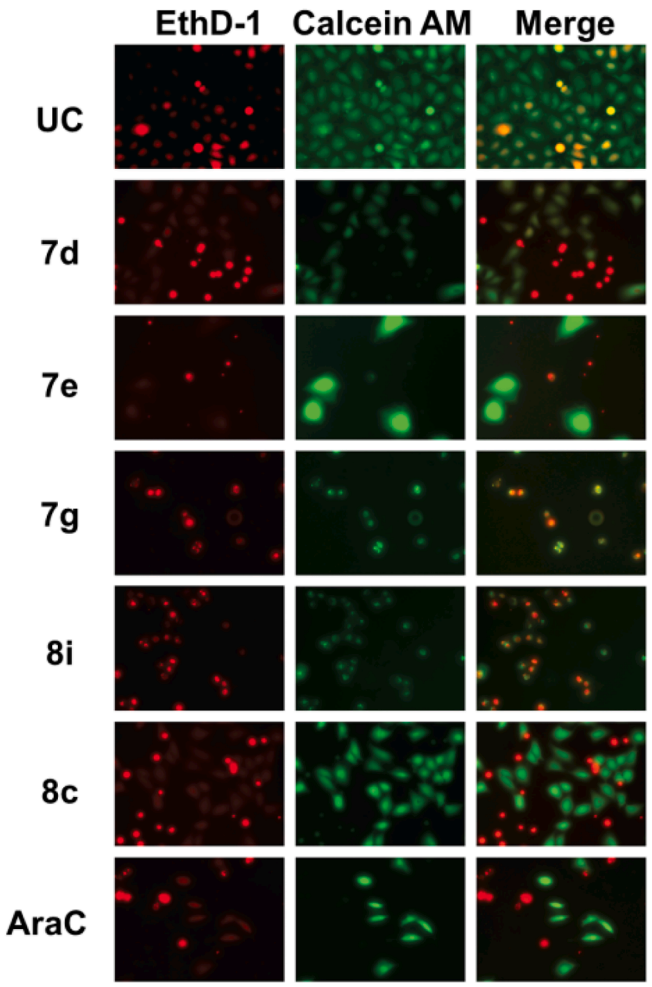

Fig. 5. The novel *N*-(4-chlorophenyl)-γ-amino acid derivatives **8c**, **7d**, **7e**, **7g**, and **8i** induces death in A549 cells. A live/dead assay were employed after A549 treatment with compounds **8c**, **7d, 7e, 7g,** and **8i** and cytosine arabinoside (AraC) for 24 h at 50 μM concentration or DMSO that served as untreated control (UC). A green fluoresence denotes viable cells stained with calcein-AM, while red/orange fluoresence represents dead cells stained with ethidium homodimer (EthD-1). (For interpretation of the references to colour in this figure legend, the reader is referred to the web version of this article.)

Furthermore, compound **7g** demosntrated the highest cytotoxicity and proliferation inhibition of A549 cells (Fig. S49 A-C). **7g** was able to signifficantly ($p < 0.005$) reduce the viability of A549 cells at the concentration of 25 μM after 24 h of treatment (Fig. S49 B). The anticancer activity of **7g** on A549 colony formation was comparable cytosine arabinoside and doxorubicin (Fig. S49 A) therefore highlighting **7g** as potencial lead for further studies.

Colectivelly, these results demonstrate that *N*-(4-chlorophenyl)-γ-amino acid derivatives possess anticancer properties while compound **7g** bearing 3,4-$Cl_2C_6H_3$ substitution shows the highest potency in inhibition of proliferation and colony formation of human A549 non-small cell lung carcinoma cells *in vitro*.

N-(4-Chlorophenyl)-γ-amino acid derivatives induces mitochondrial injury and ROS generation in A549 cells

It was previously demonstrated that numerous xenogenic amino acid derivatives are able to accumulate in mitochondria [58]. Ttherefore, we hypothesized that the cytotoxic activity of **8c, 7d, 8e, 7g** and **8i** could be a result of mitochondrial injury . To support our hypothesis we examined the microscopic changes in mitochondrial phenotypeand ROS formation in A549 cells treated with test compounds.

The A549 cells were treated with the selected and most active compounds (**8c, 7d, 8e, 7g** and **8i)** at the concentration of 50 μM for 24 h. After the treatment mitochondrial phenotype was examined by staining with MitoTracker mitochondria-specific probe [59] (Fig. 5).

The most promising *N*-(4-chlorophenyl)-γ-amino acid derivatives were able to affect the mitochondrial phenotype in A549 cells (Fig. 5). The treatment with compounds **7e, 7g** and **8i** resulted highest mitochondrial injury in comparison to untreated control (UC) or known S-phase inhibitor cytosine arabinoside (AraC) treatment (Fig. 5).

We further evaluated weather the cytotoxic activity of the compounds is leading to the ROS formation, often associated with mitochondrial injury [60–62]. The A549 cells were treated for 24 h using 50 μM of compounds **8c, 7d, 8e, 7g** and **8i** as well as AraC and DOX. Subsequently after the trreatment, the activity of superoxide dismuthase (SOD) and production of hydrogen peroxide radical was measured. The A549 treatment with compound **7d** ($p < 0.0021$) resulted significantly higher SOD activity in comparison to untreated control (UC) (Fig. 6A). Moreover, treatment with compound **7g** resulted decreased SOD activity, in comparison to UC. These results suggests that compound **7g** is capable to inducing ROS leading to the reduced SOD activity [16]. This observation was further confirmed when hydrogen peroxide radical was measured (Fig. 6B). The treatment with **7g** resulted significantly higher hydrogen peroxide production ($p < 0.0001$) in comparison to UC (Fig. 6B).

Collectively these results demonstrate that the cytotoxic activity of *N*-(4-chlorophenyl)-γ-amino acid derivatives is leading to the mitochondrial injury events resulting to elevated ROS production. Moreover, we demonstrated that 3,4-$Cl_2C_6H_3$ radical is critical, since 3,4-$Cl_2C_6H_3$

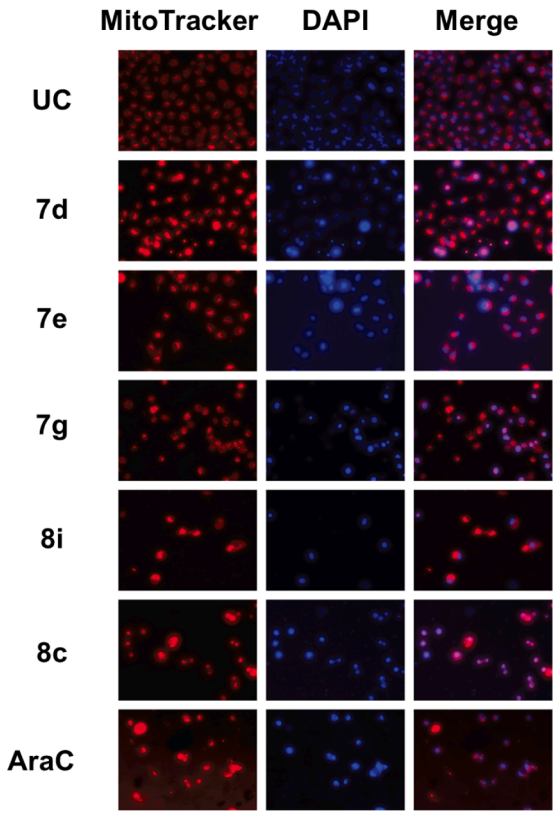

Fig. 6. The novel *N*-(4-chlorophenyl)-γ-amino acid derivatives **8c, 7d, 8e, 7g** and **8i** are able to induce the mitochondrial injury in A549 cells. The cells were treated with 50 μM of each compound or cytosine arabinoside (AraC, cytotoxicity control) and DMSO (UC, untreated control) for 24 h. After the treatment mitochondria were visualized by staining with MitoTracker red 680 while nuclei were stained with DAPI.

replacement with other groups resulted in decreased ROS production and effect on mitochondrial phenotype.

N-(4-Chlorophenyl)-γ-amino acid derivatives suppresses ATP production in A549 cells

After demonstrating that the most active *N*-(4-chlorophenyl)-γ-amino acid derivatives **8c, 7d, 8e, 7g** and **8i** are able to target mitochondria resulting ROS formation, we further evaluated weather the disruption of mitochondrial function leading to the inhibition of oxidative phosphorylation and ATP production. The A549 cells were treated with 50 μM of compounds **8c, 7d, 8e, 7g** and **8i** or cytotoxic comparators and ATP production was evaluated using colorimetric assay (Fig. 7).

All compounds except **8i** were able to significantly ($p < 0.05$ and p < 0.0021) reduce the intracellular ATP concentration, in comparison to untreated control (Fig. 7). The treatment with **7d**, **7e**, **8c** resulted in decreased intracellular ATP concentration and it was comparable to AraC treated cells (Fig. 7). Moreover, among all tested compounds, treatment with **7g** resulted in the highest ATP reduction in comparison to UC ($p < 0.0021$). The intracellular ATP levels after treatment with **7g** was also significantly lower than in AraC treated cells ($p < 0.0021$). t.

These results demonstrate that *N*-(4-chlorophenyl)-γ-amino acid derivatives can suppress oxidative phosphorylation and ATP synthesis by structure-depended manner, while 3,4-$Cl_2C_6H_3$ radical is crucial for the biological activity.

The compound 7 g enhances the cytotoxic activity of s cycle inhibitor cytosine arabinoside

We postulate that that the cytotoxic activity of S cycle inhibitor AraC could be further enhanced by using **7g** as a mitochondria-targeting compound. We hypothesized that the **7g** induced ATP starvation and profound ROS could enhance the AraC cytotoxic activity.

The A549 treatment with AraC (50 μM) alone was able to reduce the cell viability on average by 50%, while treatment with **7g** (25 and 50 μM) resulted in significant, dose-depended viability suppression in comparison to UC (Fig. 8A). The AraC (50 μM) combination with 25 μM of **7g** resulted in significantly higher reduction of A549 viability in comparison to AraC monotreatment ($p < 0.0021$). The most potent reduction of A549 viability was observed, when AraC was combined with 50 μM of **7g**. The combination therapy was able to reduce the A549 viability to 15–20% in comparison to UC or AraC monotreatment (Fig. 8A).

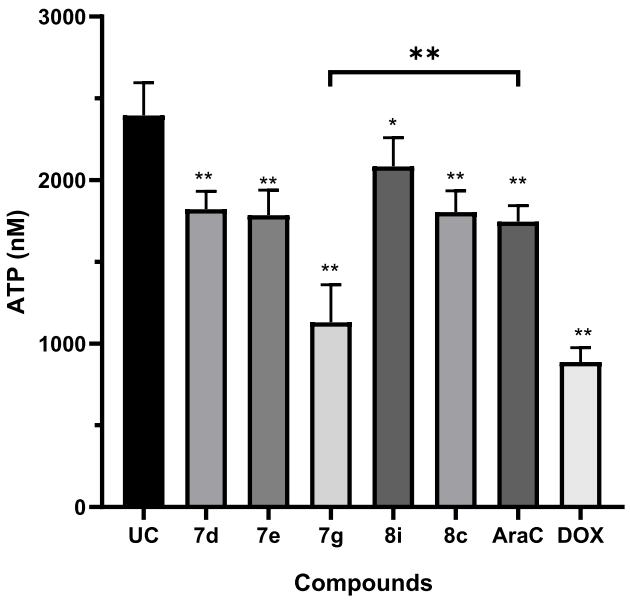

Fig. 8. The cytotoxic of *N*-(4-chlorophenyl)-γ-amino acid derivatives suppresses the intracellular ATP synthesis and oxidative phosphorylation. The A549 cells were treated with 50 μM of compounds **8c, 7d, 8e, 7g** and **8i** as well as AraC and DOX for 24 h and the intracellular ATP concentration was measured by using colorimetric assays. Statistical significance was tested with Mann-Whitney *t* test; error bars show mean ± SD from 2 experiments with 3 experimental replicas*$p < 0.05$, **$p < 0.0021$, ***$p < 0.0002$, **** $p < 0.0001$.

The AraC combination with **7g** (25 and 50 μM) resulted in significantly higher hydrogen peroxide radical formation ($p < 0.0001$) in comparison to untreated control or AraC monotreatment (Fig. 8B). Moreover, combinational treatment resulted decrease in SOD activity, therefore further suggesting the production of ROS (Fig. 8C). Furthermore, the AraC combination with **7g** was able to supress the A549 colony formation after 24 h of exposure with the compounds (Fig. 8E).

The enhanced cytotoxic effect was further confirmed by Live/Dead

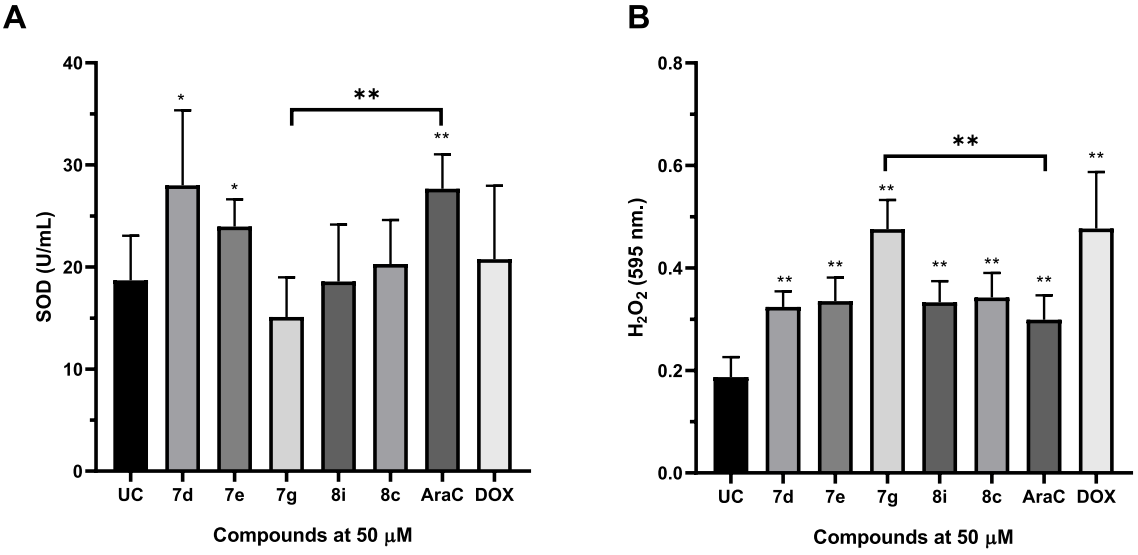

Fig. 7. The effect of cytotoxic of *N*-(4-chlorophenyl)-γ-amino acid derivatives on the superoxide dismutase (SOD) activity and hydrogen peroxide radical formation in A549 cells. The cells were treated with 50 μM of compounds **8c, 7d, 8e, 7g** and **8i** as well as AraC or DOX for 24 h and the SOD activity (A) and hydrogen peroxide production (B) was measured. Statistical significance was tested with Mann-Whitney *t* test; error bars show mean ± SD from 2 experiments containing 3 experimental replicas *$p < 0.05$, **$p < 0.0021$, ***$p < 0.0002$, **** $p < 0.0001$.

staining (Fig. 9). The AraC combination with **7g** (25 and 50 μM) resulted in increased accumulation of EthD-1 and reduction of calcein-AM staining in A549 cells in comparison to UC or AraC monotreatment. Fig. 10.

The greatest cytotoxic activity was observed when AraC was combined with 50 μM ($p < 0.0002$) (Fig. 8A).

The cytotoxic anticancer effect was observed when AraC was combined with **7g** as it was evident that A549 cells failed to formed colonies after 24 h of treatment in comparison to monotreatment with AraC or **7g** (Fig. 8 E).

After demonstrating that the AraC combination with **7g** resulting synergistic cytotoxic interactions leading to the generation of increased amount of ROS, we further evaluated weather **7g** complementation with AraC results in greater inhibition of oxidative phosphorylation leading to decreased production of cellular ATP. We showed that the AraC combination with 50 μM of compound **7g** resulted significantly lower levels of cellular ATP ($p < 0.0002$) in comparison to AraC monotherapy (Fig. 8D).

Collectively these results shows that compound **7g** synergizes with AraC-mediated anticancer activity by inducing mitochondrial damage, ROS formation and inhibition of oxidative phosphorylation. These events are leading to significant reduction of ATP production and cell death. Further studies are needed to better understand the therapeutic potential, further synergistic interactions, and cellular targets of *N*-(4-chlorophenyl)-γ-amino acid derivatives.

Conclusions

In the present study, a series of mitochondria-targeting *N*-(4-chlorophenyl)-γ-amino acid derivatives bearing azole, diazole, and triazole moieties were successfully synthesized. Additionally, we have demonstrated that the most potent compounds exert the promising anticancer activity on A549 Non-Small Cell Lung Cancer (NSCLC) cells. The *N*-(4-chlorophenyl)-γ-amino acid derivatives showed good predicted ADME and drug-like properties with good predicted gastrointestinal absorption properties, making *N*-(4-chlorophenyl)-γ-amino acid derivatives as potential orally bioavailable anticancer drugs.

Further compounds were able to induce the mitochondrial injury, leading to ROS formation and decreased ATP production. Furthermore, the compound **7g** showed synergistic interactions with cytosine arabinoside (AraC) suggesting the possible further exploration of **7g** as adjuvant in sensitizing NSCLC to standard therapy of AraC.

Mitochondria plays a vital role in cell homeostasis both in normal as well as transformed cells. Therefore, mitochondria is considered as a promising marker for anticancer therapy. Among compounds targeting mitochondria, various ubiquinone derivatives are known to interact with mitochondrial respiration complex II by competitive binding leading to mitochondrial injury and cell death. A strong complex II inhibitor α-tocopherol succinate (α-TOS) is able to compete with ubiquinone by binding Q site of respiratory chain complex II and induce the cell death in various cell lines [63].

Beside ubiquinone derivatives, various heterocyclic compounds have been previously reported to demonstrate the anticancer properties by interacting with mitochondrial pathway. Hickey *et al.* reported synthesis of novel mitochondria-targeted organometallic chemotherapeutics based on *N*-heterocyclic carbene complexes with gold [64]. The investigated compounds were highly accumulating in mitochondria and were able to induce a death in breast cancer cell lines.

The *in vitro* activity studies revealed that the most potent compounds synthesized during this study is able to induce the mitochondrial injury,

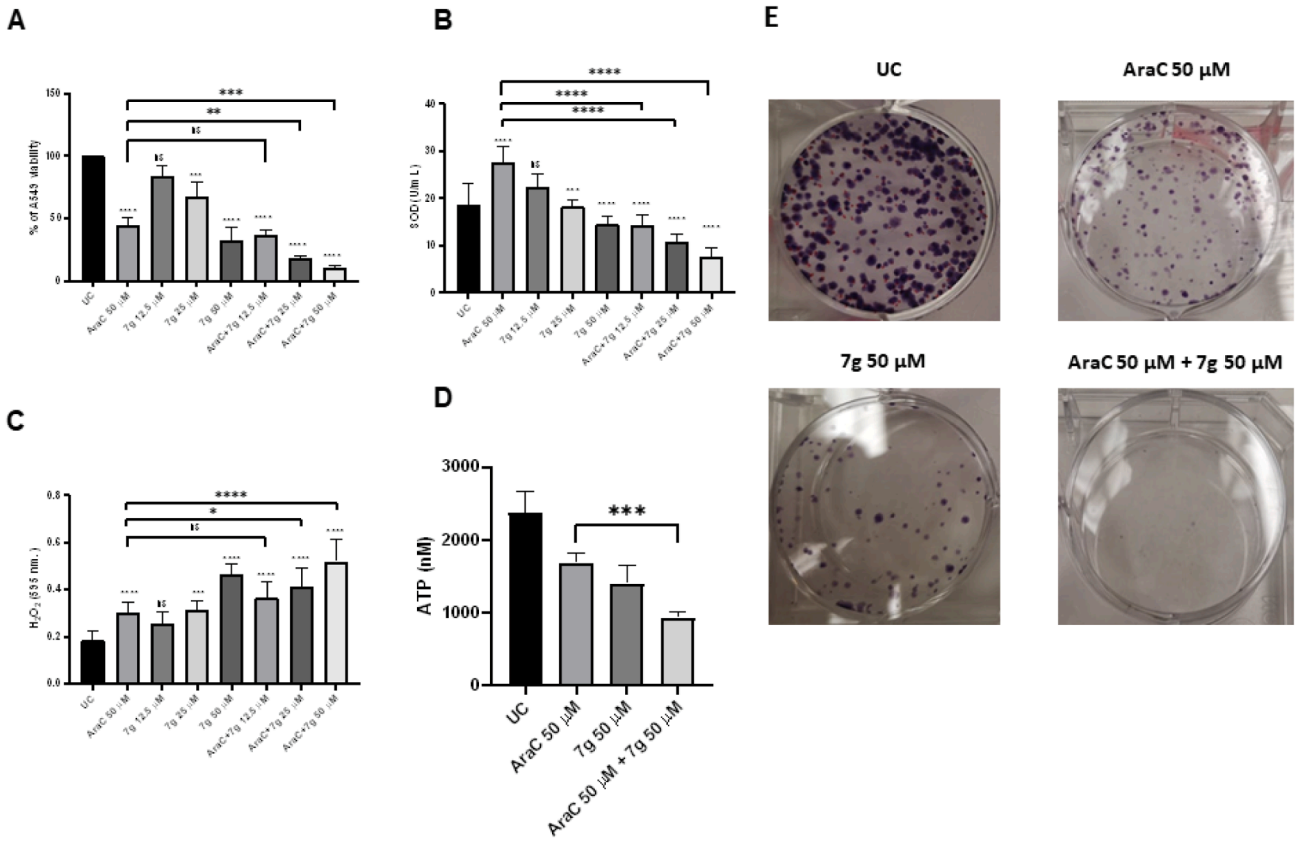

Fig. 9. The compound **7g** enhances the cytotoxic activity (panel A) of cytosine arabinoside (AraC) by inducing ROS formation (panel B and C) and inhibiting ATP synthesis (panel D) and colony formation (panel E). The A549 cells were treated with 50 μM of AraC and compound **7g** (12.5–50 μM) for 24 h. After the treatment, the viability, SOD activity, hydrogen peroxide production and ATP concentration were measured. Statistical significance was tested with one-way ANOVA test; error bars show mean ± SD from 3 experiments *$p < 0.05$, **$p < 0.0021$, ***$p < 0.0002$, **** $p < 0.0001$.

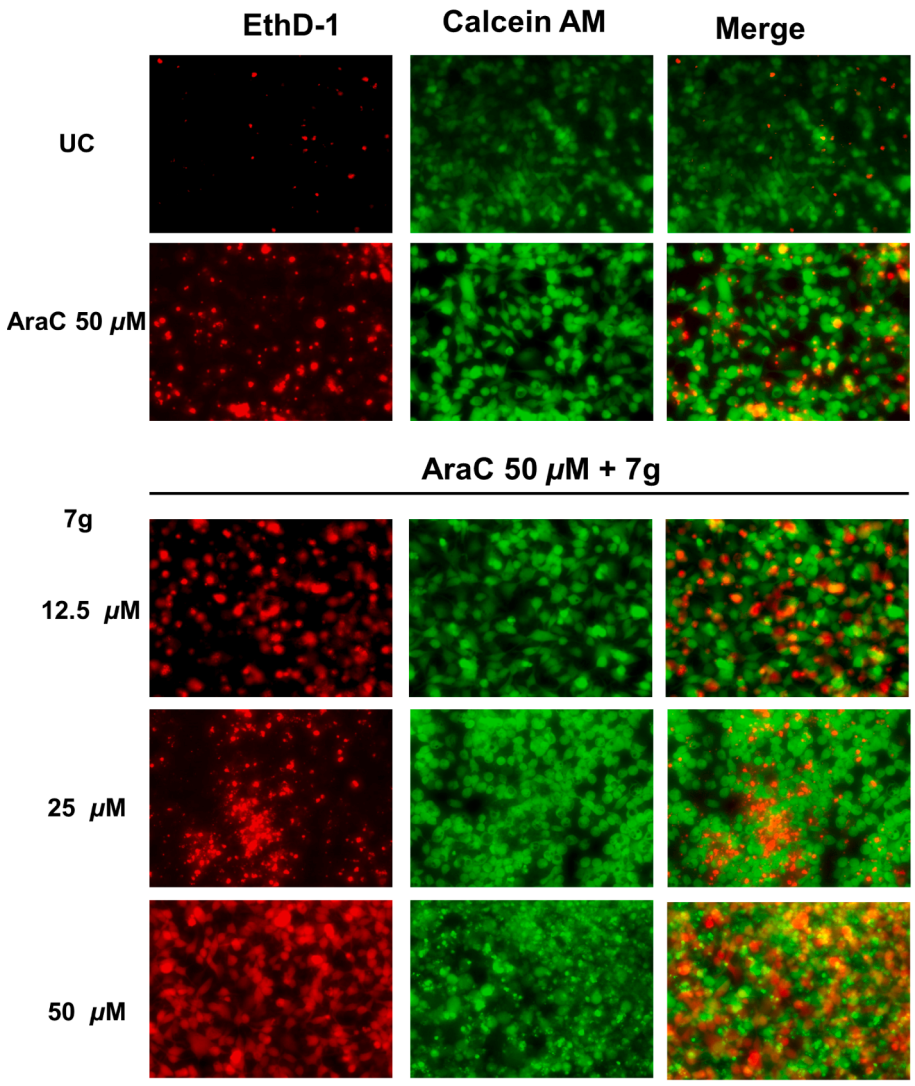

Fig. 10. The compound **7g** enhances the cytotoxic activity of cytosine arabinoside (AraC) on human A549 lung cancer cells. The A549 cells were incubated with AraC (50 μM) alone and in combination with compound **7g** (12.5–50 μM) for 24 h and the cell viability was evaluated by using Live/Dead staining. A green fluoresence denotes viable cells stained with calcein-AM, while red/orange fluoresence represents dead cells stained with ethidium homodimer (EthD-1).

as it was evident by the aberrant mitochondrial staining using selective probes. The mitochondrial injury phenotype was most evident when A549 cells were treated with **7g** (IC_{50} 38.38 μM) bearing 3,4-$Cl_2C_6H_3$ substituent. The treatment resulted in significant production of ROS as evidenced by the increase in formation of hydrogen peroxide, decrease in superoxide dismutase activity and ATP production.

Only compound **7g** synergized with AraC, suggesting that the 3,4-$Cl_2C_6H_3$ group is critical for biological activity. The synergistic combination of AraC and **7g** resulted in greater reduction of A549 viability in treated cells as well as ROS formation. The combinatory treatment resulted decreased production of ATP suggesting that the combination is acting on oxidative phosphorylation. The anticancer activity of **7g** combination with AraC was comparable to doxorubicin monotherapy, suggesting that the adverse doxorubicin associated side effects could be potentially avoided by using a combination of two drugs with additive anticancer effect.

The *in silico* prediction of ADME properties revealed that **7g** have good drug-liknes properties with Lipinski-acceptable lipophilicity, solubility and high GI absorption properties. **7g** was not predicted to be permeant through Brain-Blood barrier, therefore chemotherapy associated toxicity to CNS could be potentially avoided.

With this notion, **7g** could be further investigated as adjuvant compound enhancing cytarabine (AraC) induced killing of NSCLC. Further studies are needed to better understand the safety, *in vivo* efficacy, and cellular targets of **7g** and other anticancer *N*-(4-chlorophenyl)-γ-amino acid derivatives.

Experimental section

General procedures

Starting materials and solvents were purchased from Sigma-Aldrich (St. Louis, MO, USA) and used without further purification. The reaction course and purity of the synthesized compounds were monitored by TLC using aluminium plates pre-coated with Silica gel with F254 nm (Merck KGaA, Darmstadt, Germany). Melting points were determined with a B-540 melting point analyser (Büchi Corporation, New Castle, DE, USA) and are uncorrected. IR spectra (ν, cm^{-1}) were recorded on a Perkin–Elmer Spectrum 100 FT–IR spectrometer (Perkin–Elmer Inc., Waltham, MA, USA) using KBr pellets. NMR spectra were recorded on a Brucker Avance III (400, 101 MHz) spectrometer (Bruker BioSpin AG,

Fällanden, Switzerland). Chemical shifts were reported in (δ) ppm relative to tetramethylsilane (TMS) with the residual solvent as internal reference ([d_6] DMSO, $\delta = 2.50$ ppm for ^{1}H and $\delta = 39.5$ ppm for ^{13}C). Data are reported as follows: chemical shift, multiplicity, coupling constant [Hz], integration and assignment. Mass spectra were obtained on Bruker Daltonic – maXis 4G mass spectrometer (Bruker Daltonics, Bremen, Germany) with ESI ionization. Elemental analyses (C, H, N) were conducted using the Elemental Analyzer CE-440, their results were found to be in good agreement (±0.3%) with the calculated values.

1-(4-Chlorophenyl)-4-(5-sulfanylidene-4,5-dihydro-1H-1,2,4-triazol-3-yl)pyrrolidin-2-one (**1**, $C_{12}H_{11}ClN_4OS$). Compound **1** was synthesized according to the method described in literature [44,45].

Ethyl ({3-[1-(4-chlorophenyl)-5-oxopyrrolidin-3-yl]-1H-1,2,4-triazol-5-yl}sulfanyl)acetate (**2**, $C_{16}H_{17}ClN_4O_3S$). A mixture of triazole **1** (5.90 g, 20 mmol), ethyl chloroacetate (3.06 g, 25 mmol), and 1,4-dioxane (50 mL) was heated at reflux for 3 h. Then the reaction mixture was cooled down and diluted with water (50 mL), the precipitate was filtered off, washed with water. Recrystallization from the mixture of propan-2-ol and water (1 : 1) afforded 5.26 g (69%) **2**. M.p.: 66–67 °C; ^{1}H NMR (400 MHz, DMSO-d_6): $\delta = 13.96$ (s, 1H, NH), 7.68 (d, $J = 8.9$ Hz, 2H, H_{Ar}), 7.43 (d, $J = 8.9$ Hz, 2H, H_{Ar}), 4.24–3.93 (m, 6H, NCH_2, SCH_2, OCH_2), 3.90–3.80 (m, 1H, $CH_2\underline{CH}$), 3.02–2.75 (m, 2H, CH_2CO), 1.14 (t, $J = 7.1$ Hz, 3H, CH_3) ppm; ^{13}C NMR (101 MHz, DMSO-d_6): $\delta = 174.6$, 171.9 (2C = O), 168.7, 158.2, 138.0, 128.6, 127.9, 121.0 (C_{Ar} + 2C = N), 61.0 (OCH_2), 52.0 (NCH_2), 37.2 ($CO\underline{CH_2}$), 33.4 (SCH_2), 28.7 ($CH_2\underline{CH}$), 14.0 (CH_3) ppm; IR (KBr): $\overline{\nu} = 3520$, 1699, 1721, 1566, 1493 cm^{-1}; HRMS (ESI): *m/z* calcd. for $C_{16}H_{18}ClN_4O_3S$ $[M + H]^+$ 381.0783, found 381.0787.

4-(5-{[(1H-Benzimidazol-2-yl)methyl]sulfanyl}-1H-1,2,4-triazol-3-yl)-1-(4-chlorophenyl)pyrrolidin-2-one (**3**, $C_{20}H_{17}ClN_6OS$). A mixture of ester **2** (1.00 g, 2.63 mmol), benzene-1,2-diamine (0.60 g, 5.50 mmol) and 10% hydrochloric acid (25 mL) was heating at reflux for 48 h, cooled, diluted with water (30 mL). The precipitate was filtered off, washed with water, and dissolved in methanol, the solution was added 5% sodium carbonate (20 mL). The precipitate was filtered off, washed with water, recrystallized from methanol to afford 0.68 g (60%) **3**. M.p.: 180–181 °C; ^{1}H NMR (400 MHz, DMSO-d_6): $\delta = 13.01$ (br. s, 2H, 2NH), 7.69 (d, $J = 8.9$ Hz, 2H, H_{Ar}), 7.56–7.06 (m, 6H, H_{Ar}), 4.54 (s, 2H, SCH_2), 4.25–3.95 (m, 2H, NCH_2), 3.85 (p, $J = 7.6$ Hz, 1H, CH), 3.02–2.77 (m, 2H, CH_2CO) ppm; IR (KBr): $\overline{\nu} = 3393$, 3139, 1682, 1624, 1573, 1503 cm^{-1}; HRMS (ESI): *m/z* calcd. for $C_{20}H_{18}ClN_6OS$ $[M + H]^+$ 425.0946, found 425.0948.

2-({3-[1-(4-Chlorophenyl)-5-oxopyrrolidin-3-yl]-1H-1,2,4-triazol-5-yl}sulfanyl)acetohydrazide (**4**, $C_{14}H_{15}ClN_6O_2S$). A mixture of ester **2** (5.50 g, 15 mmol), hydrazine monohydrate (1.00 g, 20 mmol), and propan-2-ol (50 mL) was heated at reflux 5 h. Then the reaction mixture was cooled down, filtered, and washed diethyl ether. Recrystallized from methanol to afforded 3.74 g (68%) **4**. M.p.: 165–166 °C; ^{1}H NMR (400 MHz, DMSO-d_6): $\delta = 13.94$ (s, 1H, NH), 9.26 (s, 1H, CONH), 7.69 (d, $J = 8.9$ Hz, 2H, H_{Ar}), 7.43 (d, $J = 8.9$ Hz, 2H, H_{Ar}), 4.36 (br. s, 2H, NH_2), 4.24–3.97 (m, 2H, NCH_2), 3.90–3.80 (m, 1H, CH), 3.78 (s, 2H, SCH_2), 3.01–2.77 (m, 2H, CH_2CO) ppm; ^{13}C NMR (101 MHz, DMSO-d_6): $\delta = 172.1$ (C = O), 166.7 (NHC = O), 165.2, 158.4, 138.0, 128.6, 127.9, 121.0 (C_{Ar}), 52.0 (NCH_2), 37.3 ($CO\underline{CH_2}$), 33.6 (SCH_2), 29.0 ($CH_2\underline{CH}$) ppm; IR (KBr): $\overline{\nu} = 3437$, 3332, 3134, 1682, 1661, 1552, 1467 cm^{-1}; HRMS (ESI): *m/z* calcd. for $C_{14}H_{16}ClN_6O_2S$ $[M + H]^+$ 367.0740, found 367.0738.

*General procedure for the preparation of hydrazones **5a**–**e**.* A mixture of hydrazide **4** (0.37 g, 1 mmol), corresponding aldehyde (1.1 mmol), and 1,4-dioxane (10 mL) was heated at reflux for 2 h. Then the reaction mixture was cooled down, diluted with diethyl ether (20 mL). The precipitate was filtered off, washed with diethyl ether and recrystallized from methanol.

2-({3-[1-(4-Chlorophenyl)-5-oxopyrrolidin-3-yl]-1H-1,2,4-triazol-5-yl}thio)-N'-[phenylmethylidene]acetohydrazide (**5a**, $C_{21}H_{19}ClN_6O_2S$). Yield 0.31 g (68%). M.p.: 116–117 °C; ^{1}H NMR (400 MHz, DMSO-d_6): $\delta = 13.95$ (s, 1H, NH), 11.65 (s, 0.6H, CONH), 11.57 (s, 0.4H, CONH), 8.18 (s, 0.4H, N = CH), 8.00 (s, 0.6H, N = CH), 7.95–7.50 (m, 4H, H_{Ar}), 7.50–7.05 (m, 5H, H_{Ar}), 4.35 (s, 1.3H, SCH_2), 4.25–4.12 (m, 1H, NCH_2), 4.03–3.70 (m, 1H, NCH_2, 0.7H, SCH_2 and 1H, CH), 3.03–2.74 (m, 2H, CH_2CO) ppm; IR (KBr): $\overline{\nu} = 3422$, 3210, 1682, 1678, 1605, 1593, 1557 cm^{-1}; HRMS (ESI): *m/z* calcd. for $C_{21}H_{19}ClN_6O_2SNa$ $[M + Na]^+$ 477.0876, found 477.0870.

2-({3-[1-(4-Chlorophenyl)-5-oxopyrrolidin-3-yl]-1H-1,2,4-triazol-5-yl}sulfanyl)-N'-[(4-fluorophenyl)methylidene]acetohydrazide (**5b**, $C_{21}H_{18}ClFN_6O_2S$). Yield 0.35 g (74%). M.p.: 127–128 °C; ^{1}H NMR (400 MHz, DMSO-d_6): $\delta = 13.89$ (br. s, 1H, NH), 11.60 (br. s, 1H, CONH), 8.18 (s, 0.4H, N = CH), 8.00 (s, 0.6H, N = CH), 7.80–7.58 (m, 4H, H_{Ar}), 7.47–7.34 (m, 2H, H_{Ar}), 7.32–7.19 (m, 2H, H_{Ar}), 4.35 (s, 1.2H, SCH_2), 4.26–3.91 (m, 2H, NCH_2 and 0.8H, SCH_2), 3.91–3.74 (m, 1H, CH), 3.02–2.74 (m, 2H, CH_2CO) ppm; IR (KBr): $\overline{\nu} = 3437$, 3223, 1709, 1674, 1607, 1595, 1555 cm^{-1}; HRMS (ESI): *m/z* calcd. for $C_{21}H_{19}ClFN_6O_2S$ $[M + H]^+$ 473.0957, found 473.0950.

N'-[(4-Chlorophenyl)methylidene]-2-({3-[1-(4-chlorophenyl)-5-oxopyrrolidin-3-yl]-1H-1,2,4-triazol-5-yl}sulfanyl)acetohydrazide (**5c**, $C_{21}H_{18}Cl_2N_6O_2S$). Yield 0.37 g (76%). M.p.: 127–128 °C; ^{1}H NMR (400 MHz, DMSO-d_6): $\delta = 13.84$ (br. s, 1H, NH), 11.66 (br. s, 1H, CONH), 8.17 (s, 0.35H, N = CH), 8.00 (s, 0.65H, N = CH), 7.74–7.62 (m, 4H, H_{Ar}), 7.54–7.45 (m, 2H, H_{Ar}), 7.44–7.34 (m, 2H, H_{Ar}), 4.38 (s, 1.3H, SCH_2), 4.27–3.90 (m, 2H, NCH_2 and 0.7H, SCH_2), 3.92–3.77 (m, 1H, CH), 3.04–2.70 (m, 2H, CH_2CO) ppm; IR (KBr): $\overline{\nu} = 3444$, 3179, 1706, 1689, 1652, 1609, 1545 cm^{-1}; HRMS (ESI): *m/z* calcd. for $C_{21}H_{19}Cl_2N_6O_2S$ $[M + H]^+$ 489.0662, found 489.0666.

2-({3-[1-(4-Chlorophenyl)-5-oxopyrrolidin-3-yl]-1H-1,2,4-triazol-5-yl}sulfanyl)-N'-[(4-nitrophenyl)methylidene]acetohydrazide (**5d**, $C_{21}H_{18}ClN_7O_4S$). Yield 0.42 g (84 %). M.p.: 139–140 °C ; ^{1}H NMR (400 MHz, DMSO-d_6): $\delta = 13.96$ (s, 1H, NH), 11.95 (s, 0.35H, CONH), 11.87 (s, 0.65H, CONH), 8.34–8.19 (m, 0.35H, N = CH and 2H, H_{Ar}), 8.08 (s, 0.65H, N = CH), 7.91 (d, $J = 8.3$ Hz, 2H, H_{Ar}), 7.64 (d, $J = 8.8$ Hz, 2H, H_{Ar}), 7.38 (d, $J = 7.9$ Hz, 2H, H_{Ar}), 4.40 (s, 1.25H, SCH_2), 4.23–3.90 (m, 2H, NCH_2 and 0.75H, SCH_2), 3.91–3.69 (m, 1H, CH), 3.02–2.72 (m, 2H, CH_2CO) ppm; IR (KBr): $\overline{\nu} = 3457$, 3199, 1694, 1658, 1592, 1686, 1520 cm^{-1}; HRMS (ESI): *m/z* calcd. for $C_{21}H_{19}ClN_7O_4S$ $[M + H]^+$ 500.0902, found 500.0900.

2-({3-[1-(4-Chlorophenyl)-5-oxopyrrolidin-3-yl]-1H-1,2,4-triazol-5-yl}sulfanyl)-N'-[(thiophen-2-yl)methylidene]acetohydrazide (**5e**, $C_{19}H_{17}ClN_6O_2S_2$). Yield 0.30 g (65 %). M.p.: 115–116 °C; ^{1}H NMR (400 MHz, DMSO-d_6): $\delta = 13.95$ (s, 1H, NH), 11.60 (s, 0.6H, CONH), 11.54 (s, 0.4H, CONH), 8.39 (s, 0.4H, N = CH), 8.17 (m, 0.6H, N = CH) 7.74–7.58 (m, 3H, $H_{Ar+Thioph}$), 7.47–7.35 (m, 3H, $H_{Ar+Thioph}$), 7.17–7.07 (m, 1H, H_{Thioph}), 4.27 (s, 1.2H, SCH_2), 4.24–3.68 (m, 2H, NCH_2 and 0.8H, SCH_2 and 1H, CH), 3.01–2.76 (m, 2H, CH_2CO) ppm; IR (KBr): $\overline{\nu} = 3470$, 3195, 1675, 1597, 1565 cm^{-1}; HRMS (ESI): *m/z* calcd. for $C_{19}H_{17}ClN_6O_2S_2Na$ $[M + Na]^+$ 483.0440, found 483.0434.

2-[{3-(1-(4-Chlorophenyl)-5-oxopyrrolidin-3-yl)-1H-1,2,4-triazol-5-yl}thio]-N-(2,5-dimethyl-1H-pyrrol-1-yl)acetamide (**6**, $C_{20}H_{21}ClN_6O_2S$). A mixture of hydrazide **4** (0.96 g, 2.7 mmol), hexane-2,5-dione (0.34 g, 3.0 mmol), and methanol (10 mL) was heated at reflux for 3 h. Then the liquid fractions were evaporated under reduced pressure and the residue was poured over with 10% aqueous Na_2CO_3 solution (20 mL). The precipitate was filtered off, washed with water, and recrystallized from propan-2-ol to afford 0.91 g (76%) **6**. M.p.: 93–94 °C ; ^{1}H NMR (400 MHz, DMSO-d_6): $\delta = 10.46$ (br s, 2H, 2NH), 7.68 (d, $J = 8.9$ Hz, 2H, H_{Ar}), 7.42 (d, $J = 8.9$ Hz, 2H, H_{Ar}), 5.72 and 5.60 (2 s, 2H, CH-CH), 4.22–3.98 (m, 2H, NCH_2), 3.95 (s, 2H, SCH_2), 3.86–3.74 (m, 1H, CH), 3.00–2.78 (m, 2H, CH_2CO), 1.91 (s, 6H, $2CH_3$) ppm; ^{13}C NMR (101 MHz, DMSO-d_6): $\delta = 172.2$, 167.7 (2C = O), 160.8, 155.3, 138.1, 128.6, 127.8, 126.8, 120.9, 102.9 (C_{Ar}), 52.2 (NCH_2), 37.5 ($CO\underline{CH_2}$), 33.4 (SCH_2), 29.1 ($CH_2\underline{CH}$), 11.1, 10.8 ($2CH_3$) ppm; IR (KBr): $\overline{\nu} = 3329$, 3253, 1694, 1662, 1595, 1570 cm^{-1}; HRMS (ESI): *m/z* calcd. for

$C_{20}H_{22}ClN_6O_2S$ $[M + H]^+$ 445.1208, found 445.1212.

*General procedure for the preparation of compounds **7a–l**.* A mixture of triazole **2** (1.20 g, 4.1 mmol), corresponding α -haloketone (4.5 mmol), and acetone (10 mL) was heated at reflux for 2 h. The precipitate was filtered off, washed with water, and dried. Solids were dissolved in appropriate solvent, filtered and diluted with 10% aqueous sodium acetate solution.

({5-[1-(4-Chlorophenyl)-5-oxopyrrolidin-3-yl]-4H-1,2,4-triazol-3-yl} sulfanyl)acetaldehyde (**7a**, $C_{14}H_{13}ClN_4O_2S$). Yield 0.76 g (55%). M.p. 204–205 °C; ^{1}H NMR (400 MHz, DMSO-d_6): δ = 12.23 (br. s, 1H, NH), 9.55 (t, 1H, J = 5.4, CHO), 7.70 (d, 2H, J = 8.9, H_{Ar}), 7.42 (d, 2H, J = 8.9, H_{Ar}), 4.41–4.08 (m, 2H, NCH_2), 3.78 (p, 1H, J = 7.9, CH), 3.65 (d, 2H, J = 12.2, SCH_2), 3.05–2.72 (m, 2H, CH_2CO) ppm; ^{13}C NMR (101 MHz, DMSO-d_6): δ = 197.5, 172.4, 170.1 158.3, 138.2, 128.6, 127.7, 120.8, 52.2, 42.4, 37.3, 30.7 ppm; Analysis calcd. for $C_{14}H_{13}ClN_4O_2S$ (%) C, 49.93; H, 3.89; N, 16.64; Found: C, 50.03; H, 4.00; N, 16.52.

1-(4-Chlorophenyl)-4-{5-[(2-oxopropyl)sulfanyl]-1H-1,2,4-triazol-3-yl}pyrrolidin-2-one hydrochloride (**7b**, $C_{15}H_{16}Cl_2N_4O_2S$). Yield 0.89 g (56%). M.p. 162–163 °C; ^{1}H NMR (400 MHz, DMSO-d_6): δ = 10.24 (br. s, 2H, NH), 7.68 (d, 2H, J = 8.9, H_{Ar}), 7.43 (d, 2H, J = 8.9, H_{Ar}), 4.12 (s, 2H, SCH_2), 4.27–3.77 (m, 3H, CH, NCH_2), 3.02–2.73 (m, 2H, CH_2CO), 2.21 (s, 3H, CH_3) ppm; ^{13}C NMR (101 MHz, DMSO-d_6): δ = 202.4, 172.0, 160.1, 154.0, 138.0, 128.6, 127.9, 121.0, 52.0, 42.0, 37.3, 28.7 ppm; Analysis calcd. for $C_{15}H_{16}Cl_2N_4O_2S$ (%) C, 46.52; H, 4.16; N, 14.47. Found: C, 46.24; H, 4.20; N, 14.35.

4-{5-[(3-Chloro-2-oxopropyl)sulfanyl]-4H-1,2,4-triazol-3-yl}-1-(4-chlorophenyl)pyrrolidin-2-one (**7c**, $C_{15}H_{14}Cl_2N_4O_2S$). Yield 0.80 g (51%). M.p. 111–112 °C; ^{1}H NMR (400 MHz, DMSO-d_6): δ = 14.08 (br. s, 1H, NH), 7.75–7.40 (m, 4H, H_{Ar}), 5.04 (s, 2H, CH_2Cl), 4.56 (s, 2H, SCH_2), 4.34–3.91 (m, 3H, NCH_2, CH), 3.12–2.86 (m, 2H, CH_2CO) ppm; ^{13}C NMR (101 MHz, DMSO-d_6): δ = 199.2, 172.0, 156.8, 153.9, 138.0, 128.6, 127.8, 121.0, 52.0, 40.6, 37.2, 28.9, 26,9 ppm; Analysis calcd. for $C_{15}H_{14}Cl_2N_4O_2S$ (%) C, 46.76; H, 3.66; N, 14.54; Found: C, 46.58; H, 3.75; N, 14.35.

1-(4-Chlorophenyl)-4-{5-[(2-oxo-2-phenylethyl)sulfanyl]-1H-1,2,4-triazol-3-yl}pyrrolidin-2-one (**7d**, $C_{20}H_{17}ClN_4O_2S$). Yield 1.64 g (97%). M.p.: 180–181 °C; ^{1}H NMR (400 MHz, DMSO-d_6): δ = 12.26 (s, 1H, NH), 8.09–7.34 (m, 9H, H_{Ar}), 4.82 (s, 2H, SCH_2), 4.21–3.91 (m, 2H, NCH_2), 3.88–3.76 (m, 1H, CH), 2.99–2.70 (m, 2H, CH_2CO) ppm; ^{13}C NMR (101 MHz, DMSO-d_6): δ = 193.8 ($SCH_2\underline{C}O$), 172.0 (C = O), 160.3, 155.3, 138.0, 135.6, 133.6, 128.8, 128.6, 128.5, 128.4, 127.9, 121.0, 120.9 (C_{Ar}), 52.0 (NCH_2), 37.2 ($CO\underline{C}H_2$), 33.7 (SCH_2), 28.9 ($CH_2\underline{C}H$) ppm; IR (KBr): $\bar{\nu}$ = 3143, 1684, 1661, 1594, 1555 cm^{-1}; HRMS (ESI): *m/z* calcd. for $C_{20}H_{18}ClN_4O_2S$ $[M + H]^+$ 413.0834, found 413.0837.

1-(4-Chlorophenyl)-4-(5-{[2-(4-fluorophenyl)-2-oxoethyl]sulfanyl}-1H-1,2,4-triazol-3-yl)pyrrolidin-2-one (**7e**, $C_{20}H_{16}ClFN_4O_2S$). Yield 1.48 g (84 %). M.p.: 184–185 °C ; ^{1}H NMR (400 MHz, DMSO-d_6): δ = 13.91 (s, 1H, NH), 8.15–7.28 (m, 8H, H_{Ar}), 4.78 (s, 2H, SCH_2), 4.25–3.90 (m, 2H, NCH_2), 3.88–3.73 (m, 1H, CH), 2.99–2.70 (m, 2H, CH_2CO) ppm; ^{13}C NMR (101 MHz, DMSO-d_6): δ = 192.5 ($SCH_2\underline{C}O$), 172.0 (C = O), 166.4, 163.9, 158.0, 138.0, 132.3, 131.5, 131.4, 128.6, 128.5, 127.8, 120.9, 121.0, 115.9, 115.7 (C_{Ar}), 52.0 (NCH_2), 37.2 ($CO\underline{C}H_2$), 30.7 (SCH_2), 28.9 ($CH_2\underline{C}H$) ppm; IR (KBr): $\bar{\nu}$ = 3150, 1683, 1660, 1594, 1557 cm^{-1}; HRMS (ESI): *m/z* calcd. for $C_{20}H_{17}ClFN_4O_2S$ $[M + H]^+$ 431.0739, found 431.0740.

1-(4-Chlorophenyl)-4-(5-{[2-(4-chlorophenyl)-2-oxoethyl]sulfanyl}-1H-1,2,4-triazol-3-yl)pyrrolidin-2-one (**7f**, $C_{20}H_{16}Cl_2N_4O_2S$). Yield 1.35 g (74%). M.p. 184–185 °C; ^{1}H NMR (400 MHz, DMSO-d_6): δ = 13.90 (br. s, 1H, NH), 8.10–7.30 (m, 8H, H_{Ar}), 4.77 (br. s, 2H, SCH_2), 4.22–3.74 (m, 3H, CH, NCH_2), 2.89–2.70 (m, 2H, CH_2CO) ppm; ^{13}C NMR (101 MHz, DMSO-d_6): δ = 193.0, 172.0, 167.6, 158.0, 138.5, 138.0, 134.3, 130.3, 128.9, 128.6, 127.8, 120.9, 52.0, 37.2, 29.3 ppm; Analysis calcd. for $C_{20}H_{16}Cl_2N_4O_2S$ (%) C, 53.70; H, 3.61; N, 12.52. Found: C, 53.54; H, 3.48; N, 12.31.

1-(4-Chlorophenyl)-4-(5-{[2-(3,4-dichlorophenyl)-2-oxoethyl]sulfanyl}-1H-1,2,4-triazol-3-yl)pyrrolidin-2-one (**7g**, $C_{20}H_{15}Cl_3N_4O_2S$). Yield 1.44 g (73%). M.p. 148–149 °C; ^{1}H NMR (400 MHz, DMSO-d_6): δ = 13.94 (br. s, 1H, NH), 8.31–7.31 (m, 7H, H_{Ar}), 4.75 (br. s, 2H, SCH_2), 4.22–3.68 (m, 3H, CH, NCH_2), 2.66–3.02 (m, 2H, CH_2CO) ppm; Analysis calcd. for $C_{20}H_{15}Cl_3N_4O_2S$ (%) C, 49.86; H, 3.14; N, 11.63. Found: C, 49.75; H, 3.08; N, 11.51.

4-(5-{[2-(4-Bromophenyl)-2-oxoethyl]sulfanyl}-1H-1,2,4-triazol-3-yl)-1-(4-chlorophenyl)pyrrolidin-2-one (**7h**, $C_{20}H_{16}BrClN_4O_2S$). Yield 1.57 g (78%). M.p. 170–171 °C; ^{1}H NMR (400 MHz, DMSO-d_6) δ (ppm): ^{1}H NMR (400 MHz, DMSO-d_6): δ = 13.42 (br. s, 1H, NH), 7.98–7.30 (m, 8H, H_{Ar}), 4.76 (s, 2H, SCH_2), 4.22–3.74 (m, 3H, CH, NCH_2), 3.00–2.64 (m, 2H, CH_2CO) ppm; ^{13}C NMR (101 MHz, DMSO-d_6): δ = 193.2, 172.0, 160.5, 155.3, 138.0, 134.6, 131.8, 131.5, 130.3, 128.54, 127.8, 120.9, 52.0, 37.3, 28.9 ppm; Analysis calcd. for $C_{20}H_{16}BrClN_4O_2S$ (%) C, 48.85; H, 3.28; N, 11.39. Found: C, 48.71; H, 3.23; N, 11.25.

1-(4-Chlorophenyl)-4-[5-({2-oxo-2-[4-(trifluoromethyl)phenyl]ethyl} sulfanyl)-1H-1,2,4-triazol-3-yl]pyrrolidin-2-one (**7i**, $C_{21}H_{16}ClF_3N_4O_2S$). Yield 1.48 g (75%). M.p. 181–182 °C; ^{1}H NMR (400 MHz, DMSO-d_6) δ (ppm): ^{1}H NMR (400 MHz, DMSO-d_6): δ = 13.93 (br. s, 1H, NH), 8.35–7.28 (m, 8H, H_{Ar}), 4.83 (br. s, 2H, SCH_2), 4.21–3.73 (m, 3H, CH, NCH_2), 2.99–2.67 (m, 2H, CH_2CO), ppm; ^{13}C NMR (101 MHz, DMSO-d_6): δ = 193.5, 172.4, 172.0, 138.9, 138.0, 132.9, 132.6, 129.2, 128.5, 127.9, 126.1, 125.72, 125.69, 125.1, 122.4, 120.9, 52.0, 37.3, 33.7 ppm; Analysis calcd. for $C_{21}H_{16}ClF_3N_4O_2S$ (%) C, 52.45; H, 3.35; N, 11.65. Found: C, 52.37; H, 3.24; N, 11.54.

4-[({5-[1-(4-Chlorophenyl)-5-oxopyrrolidin-3-yl]-1H-1,2,4-triazol-3-yl}sulfanyl)acetyl]benzonitrile (**7j**, $C_{21}H_{16}ClN_5O_2S$). Yield 1.01 g (56%). M.p. 165–166 °C; ^{1}H NMR (400 MHz, DMSO-d_6): δ = 13.91 (br. s, 1H, NH), 8.22–7.33 (m, 8H, H_{Ar}), 4.80 (s, 2H, SCH_2), 4.21–3.73 (m, 3H, CH, NCH_2), 2.98–2.65 (m, 2H, CH_2CO) ppm; ^{13}C NMR (101 MHz, DMSO-d_6): δ = 193.5; 171.9, 138.9, 138.0, 132.7, 128.9, 128.6, 128.6, 127.8, 120.9, 120.8, 118.1, 115.4, 51.9, 37.2, 28.8 ppm; Analysis calcd. for $C_{21}H_{16}ClN_5O_2S$ (%) C, 57.60; H, 3.68; N, 15.99. Found: C, 57.48; H, 3.60; N, 15.85.

1-(4-Chlorophenyl)-4-(5-{[2-(4-nitrophenyl)-2-oxoethyl]sulfanyl}-1H-1,2,4-triazol-3-yl)pyrrolidin-2-one (**7k**, $C_{20}H_{16}ClN_5O_4S$). Yield 1.69 g (90 %). M.p.: 179–180 °C ; ^{1}H NMR (400 MHz, DMSO-d_6): δ = 13.95 (s, 1H, NH), 8.32 (d, J = 8.4 Hz, 2H, H_{Ar}), 8.21 (d, J = 8.6 Hz, 2H, H_{Ar}), 7.64 (d, J = 8.6 Hz, 2H, H_{Ar}), 7.40 (d, J = 8.4 Hz, 2H, H_{Ar}), 4.93 (s, 2H, SCH_2), 4.21–3.78 (m, 2H, NCH_2), 3.75–3.60 (m, 1H, CH), 3.01–2.64 (m, 2H, CH_2CO) ppm; IR (KBr): $\bar{\nu}$ = 3148, 1689, 1660, 1596, 1565 cm^{-1}; HRMS (ESI): *m/z* calcd. for $C_{20}H_{17}ClN_5O_4S$ $[M + H]^+$ 458.0684, found 458.0681.

1-(4-Chlorophenyl)-4-{5-[(2-{4-(methylsulfonyl)phenyl}-2-oxoethyl) thio]-1H-1,2,4-triazol-3-yl}pyrrolidin-2-one (**7l**, $C_{21}H_{19}ClN_4O_4S_2$). Yield 1.19 g (59%). M.p. 156–157 °C; ^{1}H NMR (400 MHz, DMSO-d_6): δ = 13.85 (br. s, 1H, NH), 8.29–7.35 (m, 8H, H_{Ar}), 4.83 (s, 2H, SCH_2), 4.21–3.76 (m, 3H, CH, NCH_2), 3.28 (s, 3H, CH_3), 2.68–2.97 (m, 2H, CH_2) ppm; Analysis calcd. for $C_{21}H_{19}ClN_4O_4S_2$ (%) C, 51.37; H, 3.90; N, 11.41. Found: C, 51.30; H, 3.83; N, 11.33.

*General procedure for the preparation of compounds **8a–l**.* Corresponding compound **7a–l** (2 mmol) was dissolved in acetic acid (10 mL), and several drops of sulphuric acid were added. Then the mixture was heated at reflux for 3–12 h, cooled, and pour into crashed ice (20 mL). The precipitate was filtered off, washed with water and recrystallized from methanol.

1-(4-Chlorophenyl)-4-([1,3]thiazolo[3,2-b][1,2,4]triazol-2-yl)pyrrolidin-2-one (**8a**, $C_{14}H_{11}ClN_4OS$). Yield 0.43 g (67%). M.p. 160–161 °C; ^{1}H NMR (400 MHz, DMSO-d_6): δ = 8.32 (d, 1H, J = 4.4, CH_{Th}), 7.71 (d, 2H, J = 8.8, H_{Ar}), 7.51 (d, 1H, J = 4.4, CH_{Th}), 7.42 (d, 2H, J = 8.6, H_{Ar}), 4.34–4.03 (m, 2H, NCH_2), 4.00–3.88 (m, 1H, CH_{Pyr}), 3.10–2.76 (m, 2H, CH_2CO) ppm; ^{13}C NMR (101 MHz, DMSO-d_6): δ = 172.8; 169.9, 157.4, 138.6, 129.0, 128.2, 121.4, 115.3, 52.8, 38.0, 31.0 ppm; Analysis calcd. for $C_{14}H_{11}ClN_4OS$ (%) C, 52.75; H, 3.48; N, 17.58. Found: C, 52.55; H, 3.57; N, 17.41.

1-(4-Chlorophenyl)-4-(6-methyl[1,3]thiazolo[3,2-b][1,2,4]triazol-2-

yl)pyrrolidin-2-one (**8b**, $C_{15}H_{13}ClN_4OS$). Yield 0.46 g (69%). M.p. 160–161 °C; ^{1}H NMR (400 MHz, DMSO-d_6): δ = 7.72 (d, 2H, J = 9.0, H_{Ar}), 7.42 (d, 2H, J = 9.0, H_{Ar}), 7.13 (s, 1H, CH_{Th}), 4.34–4.05 (m, 2H, NCH_2), 4.01–3.90 (m, 1H, CH_{Pyr}), 3.11–2.84 (m, 2H, CH_2CO), 2.45 (s, 3H, CH_3) ppm; ^{13}C NMR (101 MHz, DMSO-d_6): δ = 172.3; 169.1, 156.2, 138.1, 129.1, 128.5, 127.7, 120.9, 108.6, 52.4, 37.6, 30.7, 12.0 ppm; Analysis calcd. for $C_{15}H_{13}ClN_4OS$ (%) C, 54.14; H, 3.94; N, 16.84. Found: C, 54.03; H, 3.85; N, 16.78.

4-[6-(Chloromethyl)[1,3]thiazolo[3,2-b][1,2,4]triazol-2-yl]-1-(4-chlorophenyl)pyrrolidin-2-one (**8c**, $C_{15}H_{12}Cl_2N_4OS$). Yield 0.39 g (53%). M.p. 103–104 °C; ^{1}H NMR (400 MHz, DMSO-d_6): δ = 7.69 (d, 2H, J = 8.7, H_{Ar}), 7.42 (d, 2H, J = 8.8, H_{Ar}), 7.24 (s, 1H, CH_{Th}), 5.21 (s, 2H, CH_2Cl), 4.24–4.05 (m, 2H, NCH_2), 4.05–3.92 (m, 1H, CH), 2.97–2.77 (m, 2H, CH_2CO) ppm; ^{13}C NMR (101 MHz, DMSO-d_6): δ = 172.3; 169.5, 156.7, 148.5, 138.0, 128.8, 128.5, 120.9, 115.0, 52.4, 37.3, 32.9, 30.7 ppm; Analysis calcd. for $C_{15}H_{12}Cl_2N_4OS$ (%) C, 49.06; H, 3.29; N, 15.26; Found: C, 49.15; H, 3.12; N, 15.11.

1-(4-Chlorophenyl)-4-(6-phenyl[1,3]thiazolo[3,2-b][1,2,4]triazol-2-yl)pyrrolidin-2-one (**8d**, $C_{20}H_{15}ClN_4OS$). Yield 0.62 g (78 %). M.p.: 175–176 °C; ^{1}H NMR (400 MHz, DMSO-d_6): δ = 8.19 (d, J = 7.9 Hz, 2H, H_{Ar}), 7.92–7.35 (m, 8H, H_{Ar+Th}), 4.37–4.09 (m, 2H, NCH_2), 4.06–3.97 (m, 1H, CH), 3.12–2.90 (m, 2H, CH_2CO) ppm; ^{13}C NMR (101 MHz, DMSO-d_6): δ = 172.3 (C = O), 169.3, 157.2, 138.1, 131.5, 129.6, 128.9, 128.6, 127.8, 127.7, 126.3, 121.0, 110.3 (C_{Ar}), 52.5 (NCH_2), 37.6 ($CO\underline{C}H_2$), 30.8 ($CH_2\underline{C}H$) ppm; IR (KBr): $\bar{\nu}$ = 1700, 1596, 1553, 1500 cm^{-1}; HRMS (ESI): *m/z* calcd. for $C_{20}H_{16}ClN_4OS$ $[M + H]^+$ 395.0728, found 395.0728.

1-(4-Chlorophenyl)-4-[6-(4-fluorophenyl)[1,3]thiazolo[3,2-b][1,2,4]triazol-2-yl]pyrrolidin-2-one (**8e**, $C_{20}H_{14}ClFN_4OS$). Yield 0.58 g (70 %). M.p.: 151–152 °C; ^{1}H NMR (400 MHz, DMSO-d_6): δ = 8.35–7.27 (m, 9H, H_{Ar}), 4.37–4.09 (m, 2H, NCH_2), 4.03 (p, J = 6.8 Hz, 1H, CH), 3.16–2.83 (m, 2H, CH_2CO) ppm; ^{13}C NMR (101 MHz, DMSO-d_6): δ = 172.3 (C = O), 169.3, 163.8, 161.4, 157.2, 138.1, 131.3, 130.5, 128.7, 128.6, 121.0, 116.1, 115.9, 115.7, 110.1 (C_{Ar}), 52.5 (NCH_2), 37.6 ($CO\underline{C}H_2$), 30.7 ($CH_2\underline{C}H$) ppm; IR (KBr): $\bar{\nu}$ = 1689, 1596, 1560, 1510 cm^{-1}; HRMS (ESI): *m/z* calcd. for $C_{20}H_{15}ClFN_4OS$ $[M + H]^+$ 413.0634, found 413.0635.

1-(4-Chlorophenyl)-4-[6-(4-chlorophenyl)[1,3]thiazolo[3,2-b][1,2,4]triazol-2-yl]pyrrolidin-2-one (**8f**, $C_{20}H_{14}Cl_2N_4OS$). Yield 0.63 g (73 %). M.p.: 191–192 °C; ^{1}H NMR (400 MHz, DMSO-d_6): δ = 8.24 (d, 2H, J = 8.7, H_{Ar}), 7.97 (s, 1H, H_{Th}), 7.72 (d, 2H, J = 8.9, H_{Ar}), 7.64 (d, 2H, J = 8.6, H_{Ar}), 7.42 (d, 2H, J = 8.9, H_{Ar}), 4.37–3.98 (m, 3H, NCH_2, CH), 3.16–2.86 (m, 2H, CH_2CO) ppm; ^{13}C NMR (101 MHz, DMSO-d_6): δ = 172.3; 169.4, 157.2, 138.1, 134.2, 130.4, 129.0, 128.6, 127.9, 127.8, 126.5, 121.0, 120.9, 111.1, 52.5, 37.6, 30.7 ppm; Analysis calcd. for $C_{20}H_{14}Cl_2N_4OS$ (%) C, 55.95; H, 3.29; N, 13.05; Found: C, 55.76; H, 3.21; N, 13.01.

1-(4-Chlorophenyl)-4-[6-(3,4-dichlorophenyl)[1,3]thiazolo[3,2-b][1,2,4]triazol-2-yl]pyrrolidin-2-one (**8g**, $C_{20}H_{13}Cl_3N_4OS$). Yield 0.72 g (78%). M.p. 116–117 °C; ^{1}H NMR (400 MHz, DMSO-d_6): δ = 8.54–7.36 (m, 8H, CH, H_{Ar+Th}), 4.36–3.94 (m, 3H, CH_{Pyr}, NCH_2), 3.15–2.86 (m, 2H, CH_2CO) ppm; ^{13}C NMR (101 MHz, DMSO-d_6): δ = 172.3, 169.4, 157.2, 138.1, 132.0, 131.8, 131.1, 129.0, 128.6, 128.0, 127.8, 127.6, 126.1, 120.9, 112.5, 52.5, 37.7, 30.7 ppm; Analysis calcd. for $C_{20}H_{13}Cl_3N_4OS$ (%) C, 51.80; H, 2.83; N, 12.08. Found: C, 51.64; H, 2.80; N, 12.01.

4-[6-(4-Bromophenyl)[1,3]thiazolo[3,2-b][1,2,4]triazol-2-yl]-1-(4-chlorophenyl)pyrrolidin-2-one (**8h**, $C_{20}H_{14}BrClN_4OS$). Yield 0.53 g (56%). M.p. 134–135 °C; ^{1}H NMR (400 MHz, DMSO-d_6): δ = 8.25–7.31 (m, 9H, CH, H_{Ar+Th}) 4.35–3.93 (m, 3H, CH_{Pyr}, NCH_2), 3.11–2.88 (m, 2H, CH_2CO) ppm; ^{13}C NMR (101 MHz, DMSO-d_6): δ = 172.3, 169.3, 157.2, 138.1, 131.9, 130.4, 128.5, 128.1, 127.8, 126.8, 122.9, 120.9, 120.9, 111.1, 52.5, 37.6, 30.7 ppm; Analysis calcd. for $C_{20}H_{14}BrClN_4OS$ (%) C, 50.70; H, 2.98; N, 11.83. Found: C, 50.60; H, 2.89; N, 11.71.

1-(4-Chlorophenyl)-4-{6-[4-(trifluoromethyl)phenyl][1,3]thiazolo[3,2-b][1,2,4]triazol-2-yl}pyrrolidin-2-one (**8i**, $C_{21}H_{14}ClF_3N_4OS$). Yield 0.68 g (74%). M.p. 172–173 °C; ^{1}H NMR (400 MHz, DMSO-d_6): δ = 8.48–7.34 (m, 9H, CH, H_{Ar+Th}), 4.37–3.92 (m, 3H, CH_{Pyr}, NCH_2), 3.15–2.88 (m, 2H, CH_2CO) ppm; ^{13}C NMR (101 MHz, DMSO-d_6) δ = 172.3, 169.4, 157.3, 138.1, 131.3, 130.0, 129.5, 129.2, 129.1, 128.5, 127.8, 126.8, 125.8, 125.3, 122.6, 120.9, 113.0, 52.5, 37.6, 30.7 ppm; Analysis calcd. for $C_{21}H_{14}ClF_3N_4OS$ (%) C, 50.70; H, 2.98; N, 11.83. Found: C, 50.60; H, 2.89; N, 11.71.

4-{2-[1-(4-Chlorophenyl)-5-oxopyrrolidin-3-yl][1,3]thiazolo[3,2-b][1,2,4]triazol-6-yl}benzamide (**8j**, $C_{21}H_{16}ClN_5O_2S$). Yield 0.64 g (73%). M.p. 238–239 °C; ^{1}H NMR (400 MHz, DMSO-d_6): δ = 8.46–7.33 (m, 11*H*, NH_2, CH, H_{Ar+Th}), 4.38–3.92 (m, 3H, CH_{Pyr}, NCH_2), 3.13–2.90 (m, 2H, CH_2CO) ppm; ^{13}C NMR (101 MHz, DMSO-d_6): δ = 172.4, 169.4, 167.2, 157.3, 138.1, 134.8, 130.8, 130.0, 128.6, 128.0, 127.8, 126.0, 121.0, 111.8, 52.5, 37.7, 30.8 ppm; Analysis calcd. for $C_{21}H_{16}ClN_5O_2S$ (%) C, 57.60; H, 3.68; N, 15.99. Found: C, 57.41; H, 3.53; N, 15.90.

1-(4-Chlorophenyl)-4-[6-(4-nitrophenyl)[1,3]thiazolo[3,2-b][1,2,4]triazol-2-yl]pyrrolidin-2-one (**8k**, $C_{20}H_{14}ClN_5O_3S$). Yield 0.65 g (74 %). M.p.: 139–140 °C ; ^{1}H NMR (400 MHz, DMSO-d_6): δ = 8.50 (d, J = 9.0 Hz, 2H, H_{Ar}), 8.39 (d, J = 8.9 Hz, 2H, H_{Ar}), 8.24 (s, 1H, H_{Th}), 7.72 (d, J = 9.0 Hz, 2H, H_{Ar}), 7.42 (d, J = 8.8 Hz, 2H, H_{Ar}), 4.38–4.10 (m, 2H, NCH_2), 4.09–3.99 (m, 1H, CH), 3.11–2.94 (m, 2H, CH_2CO) ppm; IR (KBr): $\bar{\nu}$= 1699, 1598, 1552, 1519 cm^{-1}; HRMS (ESI): *m/z* calcd. for $C_{20}H_{15}ClN_5O_3S$ $[M + H]^+$ 440.0579, found 440.0579.

1-(4-Chlorophenyl)-4-{6-[4-(methanesulfonyl)phenyl][1,3]thiazolo[3,2-b][1,2,4]triazol-2-yl}pyrrolidin-2-one (**8l**, $C_{21}H_{17}ClN_4O_3S_2$). Yield 0.49 g (52%). M.p. 126–127 °C; ^{1}H NMR (400 MHz, DMSO-d_6): δ = 8.65–7.29 (m, 9H, CH, H_{Ar+Th}) 4.38–3.97 (m, 3H, CH_{Pyr}, NCH_2), 3.29 (s, 3H, CH_3), 3.16–2.87 (m, 2H, CH_2) ppm; ^{13}C NMR (101 MHz, DMSO-d_6): δ = 172.3, 169.5, 157.4, 141.1, 138.1, 132.1, 130.0, 128.6, 127.8, 127.7, 127.0, 121.0, 113.7, 52.5, 43.4, 37.6, 30.7 ppm; analysis calcd. for $C_{21}H_{17}ClN_4O_3S_2$ (%) C, 53.33; H, 3.62; N, 11.85. Found: C, 53.25; H, 3.57; N, 11.73.

In silico ADME prediction

The in silico absorption distribution, metabolism, and excretion (ADME) properties were predicted by using SwissADME software [54]. The SMILE structures were generated and used for ADME prediction. The physicochemical properties such as molecular weight, number of aromatic heavy atoms, Csp3 fraction, number of rotatable bonds, number of hydrogen bond acceptors and donors, molar refractivity, and total polar surface (TPSA) were predicted. The pharmacological properties, such as consensus lipophilicity (Log $P_{o/w}$), water solubility (mol/L), gastrointestinal absorption, permeability through the brain-blood barrier, interactions with P-glycoprotein 1 (Pgp) and cytochromes, and skin permeability (Log Kp) was estimated.

Cell lines and culture conditions

The non-small cell human lung carcinoma A549 cells and Vero African green monkey kidney cells were obtained from American Type Culture Collection (Rockville, MD, USA). Cells were maintained in Dulbecco's Modified Eagle Medium/Nutrient Mixture F-12 (DMEM/F-12) (Gibco, Waltham, MA, USA) supplemented with 10% fetal bovine serum (10% FBS) (Gibco, Waltham, MA, USA) and 100 U/ml penicillin and 100 μg/ml streptomycin (P/S). Cells were cultured at 37 °C humidified atmosphere containing 5% of CO_2. Cells were fed every 2–3 days and subculture upon reaching 70–80% confluence.

MTT viability assay

The remaining number of viable A549 or Vero cells after the treatment with compounds, doxorubicin, and cytosine arabinoside (cytotoxic controls) was evaluated by using commercial MTT (3-[4,5-methylthiazol-2-yl]-2,5-diphenyl-tetrazolium bromide) assay [57]. Briefly, A549 cells were plated in the flat bottomed 96-well microplates (1×10^4 cells/well) and incubated overnight to facilitate the attachment. The test compounds were dissolved in hybridoma-grade DMSO (Sigma-Aldrich, St. Louis, MO, USA) and then further serially diluted in cell culture

media containing 0.25 % DMSO to achieve a series of compound concentration (0 – 200 μM).

Subsequently, the media from the cells was aspirated and the compounds were added to the microplates. The cells were incubated at 37 °C, 5% CO_2 for 24 h. After incubation, a 10 μl of Vybrant® MTT Cell Proliferation Reagent (ThermoFisher Scientific) was added, and cells were further incubated for 4 h. After incubation, the media was aspirated, and the resulted formazan was solubilized by the addition of 100 μl of DMSO. The absorbance was then measured at 570 nm by using a microplate reader (Multiscan, ThermoFisher Scientific). The following formula was used to calculate the % of A549 viability: ([AE-AB]/[AC-AB]) × 100%. AE, AC, and AB were defined as the absorbance of experimental samples, untreated samples, and blank controls, respectively. The concentration series of 0 – 200 μM of compounds and comparators were used for the IC_{50} calculations. The experiments were performed in triplicates.

Colony formation assay

A549 cells were seeded at 6-well plates at the density of 3×10^2 cells/well and allowed to attach overnight. Then the cells were treated for 24 h with selected, most active compounds (0 – 100 μM) in media containing 0.25% DMSO. Cytosine arabinoside (AraC) and doxorubicin (DOX) ((0 – 100 μM) were used as cytotoxicity controls. After treatment, media with test compounds was aspirated, cells were washed with PBS, and then further incubated in fresh media for 10 days to facilitate the development of the colonies.

After incubation, the cells were fixed with methanol, colonies were stained with 0.5% crystal violet in 10% methanol. The surviving fraction was calculated as described as elsewhere [50]. The experiment was performed in triplicates for each test condition.

Determination of ATP production

The intracellular ATP levels were determined using colorimetric ATP Assay Kit (Sigma-Aldrich). Cells were seeded to 12-well plates at the density of 1×10^5 cells/well and incubated overnight to facilitate the attachment. Cells were subsequently treated with test compounds or comparators (DOX, AraC) at 50 μM for 24 h. After treatment, cells were washed twice with ice-cold PBS and lysed in 200 μl of ice-cold ATP assay buffer. The proteins were removed by using 10 kDa centrifugal filtration system (Micron-10 kDa, Millipore) and the samples were flash frozen by dropping in liquid nitrogen and stored at −80 °C. On the day of analysis, the samples were defrosted on ice and incubated with reaction mix for 30 min at room temperature. After incubation, the absorbance was measured at 570 nm and the ATP concentration was calculated as described by the manufacturer.

Determination of superoxide dismutase (SOD) activity

The activity of superoxide dismutase (SOD) was determined by using Invitrogen Superoxide Dismutase (SOD) Colorimetric Activity Kit (ThermoFisher Scientiffic). The A549 cells were seeded in 6-well plates at the density of 1×10^6 cells/well and incubated overnight to facilitate the attachment. Cells were subsequently treated with test compounds or comparators at 50 μM for 24 h. After incubation, the media was discarded, and the cells were washed with pre-warmed PBS. Cells were trysinized and pelleted by centrifugation at 250 × *g* for 10 min. at 4 °C. The cells were suspended in 0.5 mL of ice-cold PBS and lysed by sonication. The lysate was clarified by centrifugation at 1500 × *g* for 10 min. at 4 °C and supernatant was used for SOD assay. Prior the assay, the samples were diluted 1:4 and total SOD activity was determined as recommended my manufacturer.

Determination of hydrogen peroxide formation

The production of hydrogen peroxide was measured by using Pierce Quantitative Peroxide Assay Kit (ThermoFisher Scientiffic). The A549 cells were seeded in 6-well plates and treated with test compounds as described above. After the treatment, the cells were washed with ice-cold PBS, scarped, and suspended in 0.5 mL of ice-cold PBS. The cells were lysed by sonication and the production of hydrogen peroxide was determined as described by manufacturer.

Live/Dead assay

The qualitative microscopic evaluation of the viability of A549 cells was evaluated by using LIVE/DEAD® Viability/Cytotoxicity Kit (ThermoFisher Scientiffic). A total of 1×10^4 cells were plated on sterile coverslips and incubated overnight to facilitate the adhesion. The following day, cells were treated with test compounds at 50 μM for 24 h. The media was aspirated, and the cells were washed with PBS. Cells were stained with freshly prepared mixture of calcein-AM (2 μM) and ethidium homodimer (4 μM) (Eth-D) for 1 h. at room temperature. Images were acquired on Zeiss LSM880 confocal microscope (Germany).

Mitochondria staining

A549 cells were plated on sterile coverslips to achieve 1×10^4 cells and incubated overnight. After incubation, cells were treated with test compounds at 50 μM for 24 h and stained using 50 nM of MitoTracker red 580 for 1 h at 37 °C. After staining, cells were washed with PBS and fixed with 4% paraformaldehyde solution for 10 min. at room temperature. After fixation, cells were permeabilized with 0.1% Triton X-100 in PBS for 1 min and nuclei were stained with 300 nM of DAPI. Coverslips were mounted and images were acquired on Zeiss LSM880 confocal microscope (Germany).

Data analysis

Statistical significance was tested with Mann-Whitney *t* test or one-way ANOVA test; error bars show mean ± SD from 3 experiments $*p < 0.05$, $**p < 0.0021$, $***p < 0.0002$, $**** p < 0.0001$. All analyses were performed at GraphPad Prism software.

CRediT authorship contribution statement

Povilas Kavaliauskas: Conceptualization, Formal analysis, Investigation, Writing - original draft, Supervision. **Šarūnas Žukauskas:** Investigation, Visualization. **Kazimieras Anusevičius:** Formal analysis, Visualization, Investigation, Writing - original draft. **Benas Balandis:** Formal analysis, Investigation. **Rita Vaickelionienė:** Visualization, Investigation. **Vidmantas Petraitis:** Conceptualization, Investigation, Writing - original draft, Supervision. **Vytautas Mickevičius:** Conceptualization, Formal analysis, Writing - original draft, Supervision.

Declaration of Competing Interest

The authors declare that they have no known competing financial interests or personal relationships that could have appeared to influence the work reported in this paper.

Acknowledgment

We thank to the laboratory personnel of Kaunas University of Technology for their immense technological assistance during this study. We are thankful to Ruta Prakapaite (University of Basel, Biozentrum) for her assistance in preparation of graphical abstract and review of the paper.

Funding

This research did not receive any specific grant from funding agencies in the public, commercial, or not-for-profit sectors.

Appendix A. Supplementary data

Supplementary data to this article can be found online at https://doi.org/10.1016/j.rechem.2021.100193.

References

[1] J.R. Molina, P. Yang, S.D. Cassivi, S.E. Schild, A.A. Adjei, Non-small cell lung cancer: epidemiology, risk factors, treatment, and survivorship, Mayo Clin. Proc. 83 (2008) 584–594.

[2] R.L. Siegel, K.D. Miller, A. Jemal, Cancer statistics, CA Cancer J. Clin. 70 (2020) (2020) 7–30.

[3] V. Sosa Iglesias, L. Giuranno, L.J. Dubois, J. Theys, M. Vooijs, Drug Resistance in Non-Small Cell Lung Cancer: A Potential for NOTCH Targeting?, Front, Oncol 8 (2018) 267.

[4] M.V. Bluthgen, B. Besse, Second-line combination therapies in nonsmall cell lung cancer without known driver mutations, Eur. Respir. Rev. 24 (2015) 582–593.

[5] Y. Huang, X. Huang, C. Cheng, X. Xu, H. Liu, X. Yang, L. Yao, Z. Ding, J. Tang, S. He, Y. Wang, Elucidating the expression and function of Numbl during cell adhesion-mediated drug resistance (CAM-DR) in multiple myeloma (MM), BMC Cancer 19 (2019) 1269.

[6] G. Petroni, S.C. Formenti, S. Chen-Kiang, L. Galluzzi, Immunomodulation by anticancer cell cycle inhibitors, Nat. Rev. Immunol. 20 (2020) 669–679.

[7] W. Si, J. Shen, H. Zheng, W. Fan, The role and mechanisms of action of microRNAs in cancer drug resistance, Clin Epigenetics 11 (2019) 25.

[8] C. Abbruzzese, S. Matteoni, M. Signore, L. Cardone, K. Nath, J.D. Glickson, M. G. Paggi, Drug repurposing for the treatment of glioblastoma multiforme, J. Exp. Clin. Cancer Res. 36 (2017) 169.

[9] W.H. Lee, C.Y. Loo, M. Ghadiri, C.R. Leong, P.M. Young, D. Traini, The potential to treat lung cancer via inhalation of repurposed drugs, Adv. Drug Deliv. Rev. 133 (2018) 107–130.

[10] A. Saxena, D. Becker, I. Preeshagul, K. Lee, E. Katz, B. Levy, Therapeutic Effects of Repurposed Therapies in Non-Small Cell Lung Cancer: What Is Old Is New Again, Oncologist 20 (2015) 934–945.

[11] M. Elmeliegy, J. Den Haese, C. Talati, M. Wetzler, W.J. Jusko, Towards better combination regimens of cytarabine and FLT3 inhibitors in acute myeloid leukemia, Cancer Chemother. Pharmacol. 86 (2020) 325–337.

[12] J.P. Bewersdorf, S. Giri, R. Wang, R.T. Williams, M.S. Tallman, A.M. Zeidan, M. Stahl, Venetoclax as monotherapy and in combination with hypomethylating agents or low dose cytarabine in relapsed and treatment refractory acute myeloid leukemia: a systematic review and meta-analysis, Haematologica 105 (2020) 2659–2663.

[13] H.Y. Min, H.J. Jang, K.H. Park, S.Y. Hyun, S.J. Park, J.H. Kim, J. Son, S.S. Kang, H. Y. Lee, The natural compound gracillin exerts potent antitumor activity by targeting mitochondrial complex II, Cell Death Dis. 10 (2019) 810.

[14] D.C. WALLACE, Mitochondria and cancer: Warburg addressed, Cold Spring Harb. Symp. Quant. Biol. 70 (0) (2005) 363–374.

[15] F.A. Urra, M. Cordova-Delgado, H. Pessoa-Mahana, O. Ramirez-Rodriguez, B. Weiss-Lopez, J. Ferreira, R. Araya-Maturana, Mitochondria: a promising target for anticancer alkaloids, Curr. Top. Med. Chem. 13 (2013) 2171–2183.

[16] L. Wang, Q. Duan, T. Wang, M. Ahmed, N. Zhang, Y. Li, L. Li, X. Yao, Mitochondrial Respiratory Chain Inhibitors Involved in ROS Production Induced by Acute High Concentrations of Iodide and the Effects of SOD as a Protective Factor, Oxid. Med. Cell. Longev. 2015 (2015), 217670.

[17] J.M. Lambert, C.Q. Morris, Antibody-Drug Conjugates (ADCs) for Personalized Treatment of Solid Tumors: A Review, Adv Ther 34 (5) (2017) 1015–1035.

[18] R. Lin, P. Zhang, A.G. Cheetham, J. Walston, P. Abadir, H. Cui, Dual peptide conjugation strategy for improved cellular uptake and mitochondria targeting, Bioconjug. Chem. 26 (2015) 71–77.

[19] K. Kluckova, A. Bezawork-Geleta, J. Rohlena, L. Dong, J. Neuzil, Mitochondrial complex II, a novel target for anti-cancer agents, BBA 2013 (1827) 552–564.

[20] D.J. Newman, G.M. Cragg, N. Products, Natural products as sources of new drugs from 1981 to 2014, J. Nat. Prod. 79 (2016) (1981) 629–661.

[21] J. Jampilek, Heterocycles in medicinal chemistry, Molecules 24 (21) (2019) 3839, https://doi.org/10.3390/molecules24213839.

[22] M. Dawidowski, F. Herold, A. Chodkowski, J. Kleps, P. Szulczyk, M. Wilczek, Synthesis and anticonvulsant activity of novel 2,6-diketopiperazine derivatives. Part 1: perhydropyrrole[1,2-a]pyrazines, Eur J Med Chem, 46 (2011) 4859-4869.

[23] G.B. Liang, X. Qian, D. Feng, M. Fisher, T. Crumley, S.J. Darkin-Rattray, P. M. Dulski, A. Gurnett, P.S. Leavitt, P.A. Liberator, A.S. Misura, S. Samaras, T. Tamas, D.M. Schmatz, M. Wyvratt, T. Biftu, N-alkyl-4-piperidinyl-2,3-diarylpyrrole derivatives with heterocyclic substitutions as potent and broad spectrum anticoccidial agents, Bioorg. Med. Chem. Lett. 18 (2008) 2019–2022.

[24] J.M. Ontoria, J.I. Martin Hernando, S. Malancona, B. Attenni, I. Stansfield, I. Conte, C. Ercolani, J. Habermann, S. Ponzi, M. Di Filippo, U. Koch, M. Rowley, F. Narjes, Identification of thieno[3,2-b]pyrroles as allosteric inhibitors of hepatitis C virus NS5B polymerase, Bioorg. Med. Chem. Lett. 16 (2006) 4026–4030.

[25] S. Said Fatahala, S. Hasabelnaby, A. Goudah, G. Mahmoud, R. Helmy Abd-El Hameed, Helmy Abd-El Hameed, Pyrrole and Fused Pyrrole Compounds with Bioactivity against Inflammatory Mediators, Molecules 22 (3) (2017) 461, https://doi.org/10.3390/molecules22030461.

[26] S.J. Kaspersen, C. Sorum, V. Willassen, E. Fuglseth, E. Kjobli, G. Bjorkoy, E. Sundby, B.H. Hoff, Synthesis and in vitro EGFR (ErbB1) tyrosine kinase inhibitory activity of 4-N-substituted 6-aryl-7H-pyrrolo[2,3-d]pyrimidine-4-amines, Eur. J. Med. Chem. 46 (2011) 6002–6014.

[27] H. Kuznietsova, N. Dziubenko, I. Byelinska, V. Hurmach, A. Bychko, O. Lynchak, D. Milokhov, O. Khilya, V. Rybalchenko, Pyrrole derivatives as potential anti-cancer therapeutics: synthesis, mechanisms of action, safety, J. Drug Target. 28 (5) (2020) 547–563.

[28] G. La Regina, R. Bai, A. Coluccia, V. Famiglini, S. Pelliccia, S. Passacantilli, C. Mazzoccoli, V. Ruggieri, L. Sisinni, A. Bolognesi, W.M. Rensen, A. Miele, M. Nalli, R. Alfonsi, L. Di Marcotullio, A. Gulino, A. Brancale, E. Novellino, G. Dondio, S. Vultaggio, M. Varasi, C. Mercurio, E. Hamel, P. Lavia, R. Silvestri, New pyrrole derivatives with potent tubulin polymerization inhibiting activity as anticancer agents including hedgehog-dependent cancer, J. Med. Chem. 57 (2014) 6531–6552.

[29] M.C. Boukouvala, N.G. Kavallieratos, C.G. Athanassiou, D. Losic, L. P. Hadjiarapoglou, Y. Elemes, Laboratory evaluation of five novel pyrrole derivatives as grain protectants against Tribolium confusum and Ephestia kuehniella larvae, J. Pest. Sci. 90 (2017) 569–585.

[30] A.S. Dekhne, C. Ning, M.J. Nayeen, K. Shah, H. Kalpage, J. Fruhauf, A. Wallace-Povirk, C. O'Connor, Z. Hou, S. Kim, M. Huttemann, A. Gangjee, L.H. Matherly, Cellular Pharmacodynamics of a Novel Pyrrolo[3,2-d]pyrimidine Inhibitor Targeting Mitochondrial and Cytosolic One-Carbon Metabolism, Mol. Pharmacol. 97 (2020) 9–22.

[31] G.S. Hassan, D.E. Abdel Rahman, E.A. Abdelmajeed, R.H. Refaey, M. Alaraby Salem, Y.M. Nissan, New pyrazole derivatives: Synthesis, anti-inflammatory activity, cycloxygenase inhibition assay and evaluation of mPGES, Eur. J. Med. Chem. 171 (2019) 332–342.

[32] E. Meta, C. Brullo, M. Tonelli, S.G. Franzblau, Y. Wang, R. Ma, W. Baojie, B. S. Orena, M.R. Pasca, O. Bruno, Pyrazole and imidazo[1,2-b]pyrazole Derivatives as New Potential Antituberculosis Agents, Med. Chem. 15 (2019) 17–27.

[33] A.E. Rashad, M.I. Hegab, R.E. Abdel-Megeid, J.A. Micky, F.M. Abdel-Megeid, Synthesis and antiviral evaluation of some new pyrazole and fused pyrazolopyrimidine derivatives, Bioorg. Med. Chem. 16 (2008) 7102–7106.

[34] M.A. Abdelgawad, R.B. Bakr, H.A. Omar, Design, synthesis and biological evaluation of some novel benzothiazole/benzoxazole and/or benzimidazole derivatives incorporating a pyrazole scaffold as antiproliferative agents, Bioorg. Chem. 74 (2017) 82–90.

[35] C. Chen, J. Chen, H. Gu, N. Bao, H. Dai, Design, Synthesis, and Biological Activities of Novel Pyrazole Oxime Compounds Containing a Substituted Pyridyl Moiety, Molecules 22 (6) (2017) 878, https://doi.org/10.3390/molecules22060878.

[36] H. Dai, G. Li, J. Chen, Y. Shi, S. Ge, C. Fan, H. He, Synthesis and biological activities of novel 1,3,4-thiadiazole-containing pyrazole oxime derivatives, Bioorg. Med. Chem. Lett. 26 (15) (2016) 3818–3821.

[37] P.-C. Lv, H.-Q. Li, J. Sun, Y. Zhou, H.-L. Zhu, Synthesis and biological evaluation of pyrazole derivatives containing thiourea skeleton as anticancer agents, Bioorg. Med. Chem. 18 (13) (2010) 4606–4614.

[38] M. Pellei, V. Gandin, L. Marchiò, C. Marzano, L. Bagnarelli, C. Santini, Syntheses and Biological Studies of Cu(II) Complexes Bearing Bis(pyrazol-1-yl)- and Bis (triazol-1-yl)-acetato Heteroscorpionate Ligands, Molecules 24 (9) (2019) 1761, https://doi.org/10.3390/molecules24091761.

[39] M. Marani, A. Paone, A. Fiascarelli, A. Macone, M. Gargano, S. Rinaldo, G. Giardina, V. Pontecorvi, D. Koes, L. McDermott, T. Yang, A. Paiardini, R. Contestabile, F. Cutruzzolà, A pyrazolopyran derivative preferentially inhibits the activity of human cytosolic serine hydroxymethyltransferase and induces cell death in lung cancer cells, Oncotarget 7 (4) (2016) 4570–4583.

[40] S.A. Shahzad, M. Yar, Z.A. Khan, L. Shahzadi, S.A.R. Naqvi, A. Mahmood, S. Ullah, A.J. Shaikh, T.A. Sherazi, A.T. Bale, Jędrzej Kukułowicz, M. Bajda, Identification of 1,2,4-triazoles as new thymidine phosphorylase inhibitors: Future anti-tumor drugs, Bioorg. Chem. 85 (2019) 209–220.

[41] Z. Xu, S.J. Zhao, Y. Liu, 1,2,3-Triazole-containing hybrids as potential anticancer agents: Current developments, action mechanisms and structure-activity relationships, Eur. J. Med. Chem. 183 (2019), 111700.

[42] H.A.M. El-Sherief, B.G.M. Youssif, S.N.A. Bukhari, M. Abdel-Aziz, H.M. Abdel-Rahman, Novel 1,2,4-triazole derivatives as potential anticancer agents: Design, synthesis, molecular docking and mechanistic studies, Bioorg. Chem. 76 (2018) 314–325.

[43] S. Omar, P. Scattergood, L. McKenzie, H. Bryant, J. Weinstein, P. Elliott, Towards Water Soluble Mitochondria-Targeting Theranostic Osmium(II) Triazole-Based Complexes, Molecules 21 (10) (2016) 1382, https://doi.org/10.3390/molecules21101382.

[44] C.H. Hsieh, J.P. Wang, C.C. Chiu, C.Y. Liu, C.F. Yao, K. Fang, A triazole-conjugated benzoxazone induces reactive oxygen species and promotes autophagic apoptosis in human lung cancer cells, Apoptosis 23 (2018) 1–15.

[45] J. Ma, Y. Zhang, J. Wang, T. Zhao, P. Ji, J. Song, H. Zhang, W. Luo, Proliferative effects of gamma-amino butyric acid on oral squamous cell carcinoma cells are associated with mitogen-activated protein kinase signaling pathways, Int. J. Mol. Med. 38 (2016) 305–311.

[46] M. Amit, S. Na'ara, Z. Gil, Mechanisms of cancer dissemination along nerves, Nat. Rev. Cancer 16 (2016) 399–408.

[47] N. Kuol, L. Stojanovska, V. Apostolopoulos, K. Nurgali, Role of the nervous system in cancer metastasis, J. Exp. Clin. Cancer Res. 37 (2018) 5.

[48] S.H. Jiang, L.P. Hu, X. Wang, J. Li, Z.G. Zhang, Neurotransmitters: emerging targets in cancer, Oncogene 39 (2020) 503–515.

[49] K. Kanbara, Y. Otsuki, M. Watanabe, S. Yokoe, Y. Mori, M. Asahi, M. Neo, GABAB receptor regulates proliferation in the high-grade chondrosarcoma cell line OUMS-27 via apoptotic pathways, BMC Cancer 18 (2018) 263.

[50] V.I. Mickevičius, V. Voskienė, A. Kantminienė, K. Stasevych, M. Komarovska-Porokhnyavets, O. Novikov, V.,, Synthesis and Biological Activity of Mono- and Disubstituted 1,2,4-Triazole Derivatives, Heterocycles 81 (3) (2010) 649.

[51] R. Vaickelioniene, V. Mickevicius, Cyclization products of N-fluorophenyl-β-alanines and their properties, Chem. Heterocycl. Compd. 42 (2006) 753–760.

[52] K. Kantminienė, I. Parašotas, E. Urbonavičiūtė, K. Anusevičius, I. Tumosienė, I. Jonuškienė, R. Vaickelionienė, V. Mickevičius, Synthesis and Biological Evaluation of Novel Di- and Trisubstituted Thiazole Derivatives, Heterocycles 94 (6) (2017) 1074, https://doi.org/10.3987/COM-17-13714.

[53] M. Mickevicius, Z.J. Beresnevicius, V. Mickevicius, G. Mikulskiene, Condensation products of 1-aryl-4-carboxy- 2- pyrrolidinones with o-diaminoarenes, o-aminophenol, and their structural studies, Heteroat. Chem. 17 (2006) 47–56.
[54] A. Daina, O. Michielin, V. Zoete, SwissADME: a free web tool to evaluate pharmacokinetics, drug-likeness and medicinal chemistry friendliness of small molecules, Sci. Rep. 7 (2017) 42717.
[55] C. Rodriguez-Antona, M. Ingelman-Sundberg, Cytochrome P450 pharmacogenetics and cancer, Oncogene 25 (2006) 1679–1691.
[56] N.T.H. Nga, T.T.B. Ngoc, N.T.M. Trinh, T.L. Thuoc, D.T.P. Thao, Optimization and application of MTT assay in determining density of suspension cells, Anal. Biochem. 610 (2020) 113937, https://doi.org/10.1016/j.ab.2020.113937.
[57] K. Prabst, H. Engelhardt, S. Ringgeler, H. Hubner, Basic Colorimetric Proliferation Assays: MTT, WST, and Resazurin, Methods Mol. Biol. 1601 (2017) 1–17.
[58] P. Chandrakar, N. Gunaganti, N. Parmar, A. Kumar, S.K. Singh, M. Rashid, M. Wahajuddin, K. Mitra, T. Narender, S. Kar, beta-Amino acid derivatives as mitochondrial complex III inhibitors of L. donovani: A promising chemotype targeting visceral leishmaniasis, Eur. J. Med. Chem. 182 (2019), 111632.
[59] B. Chazotte Labeling mitochondria with MitoTracker dyes Cold Spring Harb Protoc 2011 8 2011 pdb.prot5648 pdb.prot5648.
[60] C. Guo, L. Sun, X. Chen, D. Zhang, Oxidative stress, mitochondrial damage and neurodegenerative diseases, Neural Regen Res 8 (2013) 2003–2014.
[61] M.P. Murphy, Mitochondrial dysfunction indirectly elevates ROS production by the endoplasmic reticulum, Cell Metab. 18 (2013) 145–146.
[62] D.B. Zorov, M. Juhaszova, S.J. Sollott, Mitochondrial reactive oxygen species (ROS) and ROS-induced ROS release, Physiol. Rev. 94 (2014) 909–950.
[63] J. Pourahmad, A. Salimi, E. Seydi, Natural compounds target mitochondrial alterations in cancer cell: new avenue for anticancer research, Iran, J. Pharm. Res. 13 (2014) 1–2.
[64] J.L. Hickey, R.A. Ruhayel, P.J. Barnard, M.V. Baker, S.J. Berners-Price, A. Filipovska, Mitochondria-targeted chemotherapeutics: the rational design of gold(I) N-heterocyclic carbene complexes that are selectively toxic to cancer cells and target protein selenols in preference to thiols, J. Am. Chem. Soc. 130 (2008) 12570–12571.